Beyond the tip of the seamount: Distinct megabenthic communities found beyond the charismatic summit sponge ground on an arctic seamount (Schulz Bank, Arctic Mid-Ocean Ridge)

H.K. Meyer, A.J. Davies, E.M. Roberts, J.R. Xavier, P.A. Ribeiro, H. Glenner, S.-R. Birkely, H.T. Rapp

PII: S0967-0637(22)00233-3

DOI: https://doi.org/10.1016/j.dsr.2022.103920

Reference: DSRI 103920

To appear in: *Deep-Sea Research Part I*

Received Date: 4 April 2022

Revised Date: 1 November 2022

Accepted Date: 1 November 2022

Please cite this article as: Meyer, H.K., Davies, A.J., Roberts, E.M., Xavier, J.R., Ribeiro, P.A., Glenner, H., Birkely, S.-R., Rapp, H.T., Beyond the tip of the seamount: Distinct megabenthic communities found beyond the charismatic summit sponge ground on an arctic seamount (Schulz Bank, Arctic Mid-Ocean Ridge), *Deep-Sea Research Part I* (2022), doi: https://doi.org/10.1016/j.dsr.2022.103920.

Beyond the tip of the seamount: Distinct megabenthic communities found beyond the charismatic summit sponge ground on an arctic seamount (Schulz Bank, Arctic Mid-Ocean Ridge)

H.K. Meyer*[1,2,3], A.J. Davies[4,5], E.M. Roberts[1,2,6], J.R. Xavier[1,7], P.A. Ribeiro[1,2], H. Glenner[1], S.-R. Birkely[8], and H.T. Rapp[1,2†]

1 Department of Biological Sciences, University of Bergen, PO Box 7803, 5020 Bergen, Norway

2 Centre for Deep-Sea Research, University of Bergen, PO Box 7803, 5020 Bergen, Norway

3 Institute of Marine Research, Nordnesgaten 50, 5005 Bergen, Norway

4 Center for Biotechnology and Life Sciences, University of Rhode Island, Kingston, Rhode Island 02881, USA

5 Graduate School of Oceanography, University of Rhode Island, Narragansett 02882, USA

6 School of Ocean Sciences, Bangor University, Menai Bridge, Anglesey LL59 5AB, UK

7 CIIMAR – Interdisciplinary Centre of Marine and Environmental Research, University of Porto, 4450-208 Matosinhos, Portugal

8 Institute of Marine Research (IMR), Fram Centre, Langnes, P.O Box 6606, 9296 NO-Tromsø, Norway

*Corresponding author: heidi.kristina.meyer@hi.no

† Deceased

Abstract

Our understanding of the benthic communities on arctic seamounts and descriptions of such communities in habitat classification systems are limited. In recent years, Schulz Bank (73°52'N 7°30'E), a seamount on the Arctic Mid-Ocean Ridge (AMOR), has become well studied but the work has primarily focused on an arctic sponge ground at the summit. This has compounded a general assumption that the most biologically interesting community is on the summit alone. With the potential threat of deep-sea mining on nearby sites on AMOR, it is crucial to form a baseline understanding of the benthic megafaunal communities not only on the summit, but on the slopes and base of the seamount as well. Using video footage collected by a remotely operated vehicle in 2017 and 2018 to survey the seamount from 2700 to 580 m depth, several distinct megafauna communities on Schulz Bank were identified. Specifically, five biotopes, two of which were

dominated by large structure-forming sponges, appeared to follow a depth gradient and change with the type of substrata present. The sponge-dominated communities on the summit and lower slope had the highest average community densities and number of morphotaxa per image compared to the upper slope and seamount base communities. Most notably, sponge-dominated bedrock walls on the lower slopes challenge the assumption that the summit is the most dense and diverse community on Schulz Bank. The results from this study lay the foundation for future research and conservation efforts of arctic sponge grounds by looking beyond the seamount summit to bring a full view of enigmatic sponge dominated ecosystems.

Keywords:
Deep-sea, Biotope, Ostur, Remotely operated vehicle

1. Introduction

Seamounts are elevated geomorphological features (e.g., mountains, volcanoes, knolls, hills) that make up approximately 20% of the seafloor (Clark et al., 2021, 2010; Costello et al., 2020; Yesson et al., 2011). Their topographic complexity, large depth gradient (hundreds to thousands of meters above the seafloor), diverse substrata, and influence on the local hydrodynamic regime can promote the formation of rich and structurally-complex megabenthic communities (e.g., cold-water coral reefs, coral gardens, or sponge grounds) on their slopes and summits (Baco, 2007; Clark et al., 2021; Ramiro-Sánchez et al., 2019; Rogers et al., 2007; Samadi et al., 2007). These communities are frequently classified as Vulnerable Marine Ecosystems (VMEs) because of their uniqueness or rarity, long-living and slow-growing nature, structural complexity, functional significance, and susceptibility to anthropogenic disturbances (FAO, 2009; Samadi et al., 2007; Watling and Auster, 2021). Seamount communities can have high variation in species richness and composition and are often correlated with abiotic conditions (e.g., water mass structure, substrata, food availability, etc.) (Bridges et al., 2021; Clark et al., 2010; Goode et al., 2021; Victorero et al., 2018). While research on seamounts has occurred in all oceans, few have focused on those in arctic regions (Clark et al., 2021).

Recent research on arctic seamounts has concentrated primarily on Schulz Bank (73°52’N 7°30’E), a pristine seamount on the Arctic Mid-Ocean Ridge (AMOR) accommodating a diverse and dense arctic sponge ground at the summit (Busch et al., 2020; Hanz et al., 2022, 2021; Meyer

et al., 2019; Morrison et al., 2020; Roberts et al., 2018). Previous studies of Schulz Bank described the dominant taxa in the summit sponge ground (Meyer et al., 2019; Morrison et al., 2020) and explored the trends in sponge density with increasing water depth to about 1300 m (Roberts et al., 2018). The summit is covered by a dense spicule mat and inhabited by large structure-forming sponges, soft corals, anemones, ascidians, small crustaceans, echinoderms, and demersal fish – some of which use this sponge ground as a nursery area (see Meyer et al., 2019). Many of the large sponge species found on Schulz Bank have also been classified as indicator species of arctic sponge VMEs, based on the ICES VME indicator lists (ICES, 2020), such as hexactinellids (genera *Asconema*, *Trichasterina*, *Schaudinnia*, and *Scyphidium*), large demosponges (*Geodia hentscheli* Cárdenas, Rapp, Schander & Tendal, 2010, *Geodia parva* Hansen, 1885, and *Stelletta rhaphidiophora* Hentschel, 1929), and smaller demosponges (genera *Craniella* and *Thenea*), and for slope communities – *Lissodendoryx (Lissodendoryx) complicata* (Hansen, 1885) (Cárdenas et al., 2013; ICES, 2020; Klitgaard and Tendal, 2004; Maldonado et al., 2016; Mayer and Piepenburg, 1996; Murillo et al., 2018). However, the megafaunal communities along the slopes and base of Schulz Bank have yet to be described, and the extent of the summit sponge ground and associated megafauna is still unknown.

Commercially relevant species, such as the Greenland Halibut (*Reinhardtius hippoglossoides* (Walbaum, 1792)), inhabit the summit and to the best of our knowledge, this seamount has been subjected to limited direct anthropogenic disturbances in the past (Bowering and Nedreaas, 2000; Meyer et al., 2019; Morrison et al., 2020). According to the Global Fishing Watch, from 2012 to 2022 Schulz Bank has had relatively limited bottom fishing efforts on the seamount itself, however the immediate area surrounding the seamount has been targeted previously (see globalfishingwatch.org/map/). The majority of the increased bottom fishing efforts near Schulz Bank occurs south of the seamount and AMOR (between 71°43’N 2°17’E to 72°8’N 9°59’E horizontally and 73°8’N 7°39’E to 72°8’N 7°28’E vertically).

Schulz Bank is, however, located in proximity to a number of hydrothermal vent fields containing seafloor massive sulphide deposits along the ridge (see Figure 1) (Pedersen et al., 2010a, 2010b; Pedersen and Bjerkgård, 2016). As such, the area has attracted commercial and scientific interest in light of its deep-sea mining potential, and much of AMOR falls within the Norwegian bottom area exclusive economic zone (EEZ) (Oljedirektoratet, 2021; Pedersen et al., 2021). In recent years, the Norwegian Petroleum Directorate (NPD) was tasked by the Norwegian

Government to identify areas with mineral deposits (e.g., seafloor massive sulphide deposits and manganese crusts) on AMOR. During these operations, NPD has been focusing on known active and inactive hydrothermal sites (e.g., Loki's Castle, Mohn's Treasure, and Ægir) and expanding their mapping to other unexplored seamounts and vent sites (Pedersen et al., 2010b, 2010a, 2021; Pedersen and Bjerkgård, 2016). Norway will likely be opening for mining exploration in the coming years (estimated to be as early as 2023), even though there is still limited information regarding the AMOR benthic communities and their potential vulnerability to deep-sea mining (Oljedirektoratet, 2021). While there has been an increased effort to overcome knowledge gaps of benthic and microbial communities on AMOR (Eilertsen et al., 2018, 2020; Jaeschke et al., 2012; Kongsrud et al., 2017; Pedersen et al., 2010a; Ramirez-Llodra et al., 2020; Schander et al., 2010), the baseline understanding of hydrothermal and seamount communities on AMOR is still limited. Furthermore, the potential effect of deep-sea mining is still not well-understood, and possible impacts (e.g., sediment plumes) may not be restricted to the targeted areas (Boschen et al., 2013; Miller et al., 2018). It is suspected, however, that the outcomes would be similar to or greater than those caused by bottom trawling (Clark et al., 2010).

Deep-sea habitat studies often place greater emphasis on biologically interesting regions (i.e., regions with specific benthic or topographic features that tend to contain certain species or communities) over exploring areas that may lack the species or communities of direct interest. For seamounts, these areas tend to be summits and upper slopes, as they often host diverse and charismatic communities (typically VMEs) with key taxa of interest (e.g., cold-water coral reefs, coral gardens, or sponge grounds) due to the local hydrodynamics (Baco, 2007; Bridges et al., 2021; Clark et al., 2010; Perez et al., 2018; Ramos et al., 2016; Rogers, 2018). However, by only focusing on regions of assumed biological interest, it can be easy to overlook nearby communities that may have significant importance, ecologically or through connectivity, or be susceptible to anthropogenic disturbances targeting nearby locations, which may be the case with deep-sea mining (Miller et al., 2018). For example, a barite field hosting dense siboglinid tube worm (*Sclerolinum contortum* Smirnov, 2000) and microbial communities was discovered outside the main venting field at Loki's Castle (Pedersen et al., 2010a; Steen et al., 2016), a hydrothermal vent field just east of Schulz Bank on AMOR. These communities have been found to be biologically unique and more diverse than the actual vent field communities, further highlighting the need to expand the point of view when surveying the deep-sea. Without a representative baseline

understanding of the communities in (and near) areas of interest, establishing the true impact of anthropogenic disturbances on benthic communities becomes challenging.

Describing and classifying biotopes or the associated morphotaxa community within a specific habitat (Costello, 2009; Costello et al., 2020) is a necessary precursor for high quality habitat mapping and the design of effective management plans (Davies et al., 2015). Biotopes are generally defined as the dominant species as well as the physical environment (e.g., depth range, dominant substratum) (Buhl-Mortensen et al., 2020; Costello, 2009). To date, arctic sponge ground biotopes lack clear classification in many habitat classification systems, such as the European Nature Information System (EUNIS), likely due to the lack of knowledge and research on these communities. In addition, EUNIS classifications that incorporate seamounts are also limited to the summit and upper slopes (EUNIS, 2019), which completely excludes communities on the lower slopes and seamount base. As such, accurate habitat maps at the resolution needed for the conservation and distribution modeling of arctic sponge grounds are not yet available but urgently needed. In this study, we extend the view of Schulz Bank by asking "which megafaunal biotopes, including the arctic sponge ground biotope at the summit, does Schulz Bank support?"

The primary objectives of this study are to: 1) identify and classify the main benthic megafaunal biotopes on Schulz Bank together with their respective depth ranges and dominant substrata; 2) investigate the trends within and across biotopes; and 3) describe the community structure within each biotope further identifying the characterising megafauna. This study describes the overall Schulz Bank benthic megafaunal communities from the base to the summit and identifies communities that have been previously overlooked on Schulz Bank. The results from this study lay the foundations for exploring drivers of community structure and distribution in the future. In addition, it forms a baseline against which any potential future changes can be assessed in light of climate change, deep-sea mining, and other anthropogenic impacts.

2. Methods

2.1.Site Description

Schulz Bank is a seamount on AMOR, located at the transitional point of the Mohn Ridge into the Knipovich Ridge (Figure 1). It has a large depth gradient, from 580 m at the summit to more than 2700 m at the base. The seamount is influenced by three water masses: the warmer and more saline Norwegian Atlantic Water above the seamount, and the colder and fresher Norwegian Arctic

Intermediate Water, influencing the summit and upper slopes, and Norwegian Deep Water on the slopes and base (Hopkins, 1991; Jeansson et al., 2017; Roberts et al., 2018). The summit of Schulz Bank is subjected to internal waves (Hanz et al., 2021; Roberts et al., 2018), where the average current speed at the summit is 0.14 m s^{-1} with daily fluctuations of ~0.40 m s^{-1} and can reach up to 0.72 m s^{-1} in the winter (Hanz et al., 2021). Further description of the Schulz Bank short and long-term oceanographic setting can be found in Roberts et al. (2018) and Hanz et al. (2021).

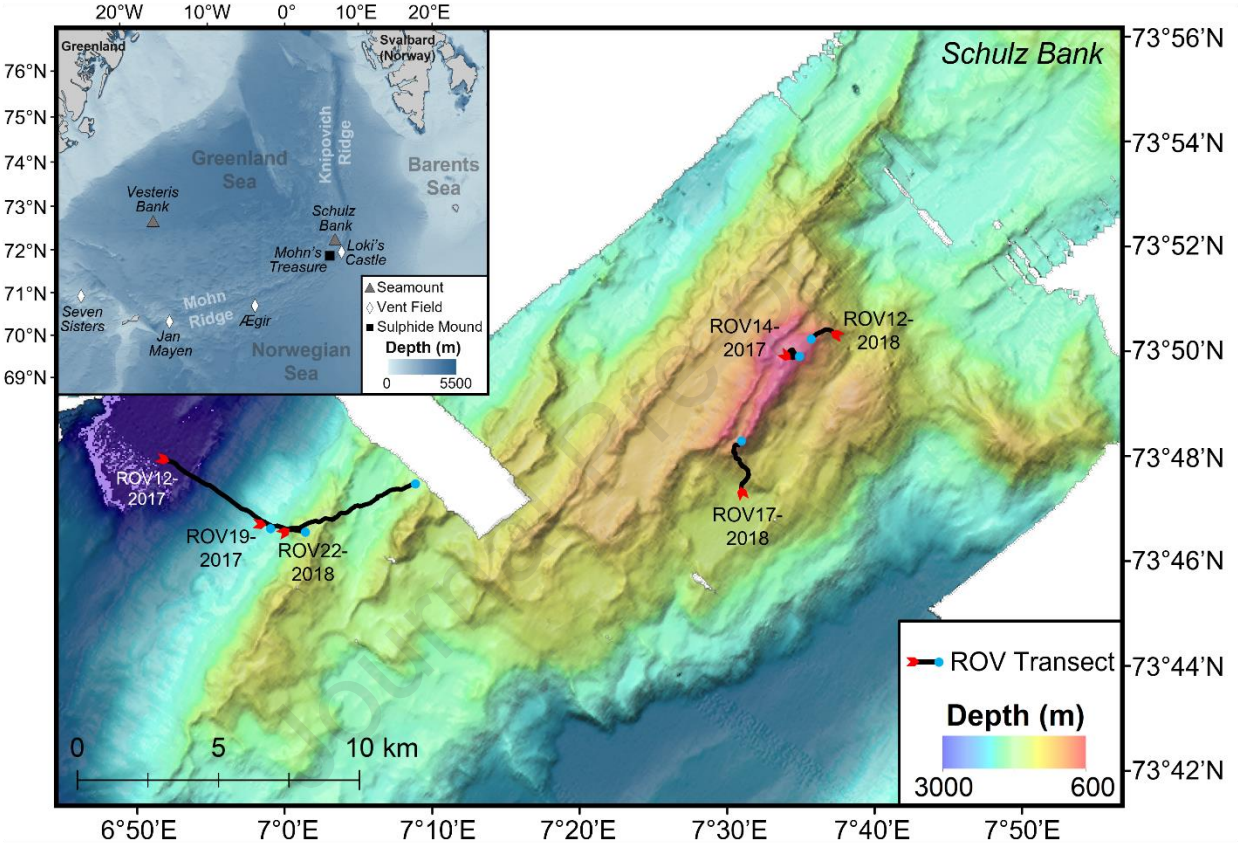

Figure 1. Bathymetric map of Schulz Bank with an inset showing location of Schulz Bank, Vesteris Bank, vent fields, and sulphide mounds on the AMOR relative to Greenland, Norway, and Svalbard. The inset's digital bathymetry has a resolution of 1/16 x 1/16 arc min and was extracted from EMODnet Bathymetry Consortium (2020). The locations of the ROV *Ægir6000* video transects are indicated by the black lines, where the red arrow and blue dot on the transect lines indicate starting and ending position, respectively. Further information about each ROV transect is presented in Table 1. The bathymetry survey was conducted on R.V. *G.O. Sars* using a Kongsberg EM 302 multibeam echosounder in 2016 (data provided by the Centre for Deep Sea Research, University of Bergen, Norway). The total area of the seamount rising from the seafloor is approximately 280 km^2.

2.2. Collection process

High-resolution video footage of Schulz Bank was collected by the remotely operated vehicle (ROV), *Ægir6000* (Kystdesign AS, Haugesund, Norway), during the SponGES project cruises on

the *R.V. G.O. Sars* in the summers of 2017 and 2018. *Ægir6000* is a work-class ROV specifically equipped for scientific surveys, with a depth rating of 6000 m. *Ægir6000* navigates using high performance subsea inertial navigation system, where it is equipped with a Linkquest Doppler Velocity log and an iXBlue PHINS 6000 Gyro and Compass. It is mounted with two Imenco Spinner II Shark Wide Angle 3G HD-SDI cameras with a zoom capacity of 30x and a resolution of 1080p at 60fps. In the water, the angle of view of the cameras are 72° diagonally and 65° horizontally. One camera is positioned towards the top of the ROV, and the other is positioned directly above the lasers at the center of the ROV. Due to the positioning relative to the lasers and the fact that the center camera was more consistently downward facing (whereas the top camera was used primarily for navigation), the center camera was selected for annotation. The distance between the laser pointers was set to 16 cm for all dives. The dives chosen for this study were dedicated transect dives (as opposed to dives that focused on biological sampling, gear deployment, or had mixed purposes), resulting in a total of 6 ROV dives being annotated (Table 1).

Table 1. The metadata of the ROV *Ægir6000* video transects and the selected images. Transect start and end positions were obtained from the respective dive logs and approximate transect length were measured in ESRI ArcGIS Desktop 10.6 (ESRI, 2017).

Dive-year	Transect start (lat., long.)	Transect end (lat., long.)	Transect length (m)	Image depth (m) range	No. of images	Image area (m^2)
ROV 12-2017	73.7904, 6.8545	73.7705, 6.9737	4335	2775–2172	141	382.39
ROV 14-2017	73.8296, 7.5595	73.8311, 7.5617	4824	586–579	73	380.66
ROV 19-2017	73.7709, 6.9726	73.7695, 7.010	1175	2072–1669	111	295.70
ROV 12-2018	73.8380, 7.6052	73.8360, 7.5852	787	817–682	61	213.02
ROV 17-2018	73.7869, 7.5069	73.8011, 7.5037	2130	1485–687	182	518.75
ROV 22-2018	73.7709, 6.9985	73.7856, 7.1334	4623	1769–1557	32	103.97

Physical specimens were opportunistically collected during the ROV dives to confirm some fauna identities. The collected fauna were identified by some of the authors (Rapp, Xavier, and Ribeiro) during and post cruise. Physical specimens were preserved in 99% ethanol and added to the collections of the University of Bergen, Norway.

2.3.Image annotation

Images were extracted from the videos using VLC Media Player at approximately one-minute intervals to reduce the possibility of spatial overlap between images. The distances between images were checked in ArcGIS Desktop 10.6 (ESRI, 2017) to ensure spatial separation by at least 1 m. This resulted in 3 images being dropped from analysis due to them having a separation less than 1 m to corresponding images. Images were initially cropped in R studio (version 4.0.2; package: magick, version 2.6.0 (Ooms, 2021)) to reduce distortion around the image edges.

Image annotation took place in the online image and video annotation software BIIGLE 2.0 (Langenkämper et al., 2017). From the cropped images, image area was calculated automatically based on setting the laser separation to 16 cm and extracting the image metadata within BIIGLE 2.0. Images retained for annotation fulfilled the following criteria: 1) both laser points were visible; 2) cropped image area ranged between 1.5 and 6 m^2; 3) images were of good quality (e.g., downward facing, not blurry or dimly exposed, not obstructed by sediment or ROV equipment); and 4) taken only during periods of transit and not while collecting or inspecting fauna.

Each image was initially given a substratum category visually determined by the most dominant substratum present within the image and based on the Wentworth (1922) substrata categories: bedrock, cobble, pebble, soft sediment, as well as mixed sediment and spicule mat. Mixed sediment was classified as a substratum that contained soft sediment covered in rod-like biogenic material (that was not spicule mat) (see supplementary materials S1).

All annotations were checked to confirm that identifications were correct and consistent between the ROV dives due to possible differences in image quality (e.g., lighting, camera angle, resolution, etc.) between years and localities using the Label Review Grid Overview (Largo) evaluation tool in BIIGLE 2.0. Largo evaluation puts all annotations with a particular label in a grid to examine if the annotations are morphologically consistent or if outliers are present (Langenkämper et al., 2017), in which case they can be changed to a different label or removed all-together if they are not part of the label set.

2.4.Fauna identification

All individuals larger than 1 cm were counted in each image, which is common in many visual-based surveys (Durden et al., 2016). Fauna were identified to the lowest taxonomic level possible

and given their own unique identification number. Fauna from the video footage that had uncertain identifications were checked by the co-authors (Meyer, Rapp, Xavier, Ribeiro, Glenner, and Birkely) and other experts (see acknowledgements), although in many cases the specimens were not able to be identified to species level. Specimens that could not be identified to species or genus level, were assigned to higher taxonomic ranks or morphotaxa and combined with open nomenclature signs as proposed by Horton et al. (2021) (e.g., Ophiuroidea indet. 60, White Encrusting Sponge 133, *Ascidia obliqua* Alder, 1863 inc. 19, etc.). Due to the difficulty of separating two of the larger demosponge species without examining physical specimens, *Geodia parva* and *Stelletta rhaphidiophora* were classified as *Geodia parva / Stelletta rhaphidiophora* 211 in the identification process. Similarly, three large rossellid glass sponges present in the sponge ground were grouped into one class – *Schaudinnia rosea* (Fristedt, 1887) / *Trichasterina borealis* Schulze, 1900 / *Scyphidium septentrionale* Schulze, 1900 213 (referred to as Hexactinellida spp. in Meyer et al. 2019 and Morisson et al., 2020). Encrusting or branching organisms were particularly difficult to count, therefore their abundance was expressed as number of encrusting groups, clusters, or clumps rather than individuals (e.g., *Lissodendoryx (Lissodendoryx) complicata* 114, *Hexadella dedritifera* Topsent, 1913 110, *Isidella* sp. indet. 39, etc.).

2.5.Statistical analysis

2.5.1. Data preparation

The abundance data was converted to density (ind. m^{-2}) for each image. To ensure that the analyses focused primarily on the reliably sampled morphotaxa and were not heavily influenced by rare morphotaxa, morphotaxa that had a density lower than 0.01% of the total megafaunal density were removed from the analyses. This resulted in all fish and many mobile taxa being dropped from the analyses. Seven additional images were dropped from the analysis due to the complete lack of fauna in those images after rare taxa were excluded. In total, 600 images were included in the analysis and covered an area of 1891.5 m^2.

2.5.2. Community analyses

All multivariate statistics were conducted in PRIMER-E version 7 (Clarke and Gorley, 2015). To account for the presence of a few highly abundant taxa (e.g., ascidians, actiniarians, ophiuroids, etc.), the raw density data was square-root transformed (Field et al., 1982). The type of

transformation used was determined while exploring the data with shade plots (supplementary materials S2) (Clarke and Gorley, 2015).

A Bray-Curtis similarity matrix was applied to the transformed dataset to summarize and compare the overall similarity between the images (Field et al., 1982), giving more weight to highly abundant morphotaxa than to the rarer ones. A linkage tree cluster analysis was conducted to identify the main biotope types on the seamount and incorporated dominant substratum and 100 m depth intervals to help distinguish the clusters (Clark and Gorley, 2015). Converting depth to 100 m depth intervals was chosen to ensure images had comparable depth ranges. The divisions of the y axis were displayed at the split quality (B%) level to examine the magnitude of the differences within the cluster dendrogram, where the lower the B% the more similar the images are to one another within that cluster (Clark and Gorley, 2015).

However, due to the arbitrary fitting of cluster dendrograms (Field et al., 1982), a non-metric Multi-Dimensional Scaling (nMDS) ordination plot was generated to visualize how close the images within the biotopes were clustering, i.e., how similar the images were within that biotope. This was done to confirm the trends observed in the linkage tree dendrogram (Field et al., 1982). The dominant substratum was superimposed on the nMDS to visualize the main substratum transitions within and between the biotopes. To ensure the dataset was consistent between 2017 and 2018, the megafauna density and number of morphotaxa from each dive as well the nMDS with the dive numbers superimposed on the ordination plot was used to compare the communities between dives (supplementary materials S3).

After the biotopes were identified, species rarefaction curves were generated on the untransformed density data to assess the morphotaxa richness within the biotopes. While this type of analysis rarely reaches the asymptote for megafaunal assemblages, species rarefaction curves may be used to compare the differences in species richness within communities (Gotelli and Colwell, 2001).

A Similarity Percentage (SIMPER) analyses was conducted to investigate the community structure within each biotope and identify the main taxa contributing most to the similarity within and between the biotopes. Morphotaxa that were consistently driving the most similarity within and between the biotopes were considered characterising morphotaxa (Clarke and Gorley, 2015; Mayer and Piepenburg, 1996). This is determined by the (dis)similarity and standard deviation ratio (sim/sd), where the larger the ratio within and between the biotopes, the more consistent the

morphotaxa are contributing to the distinctions of the biotopes (Clarke and Gorley, 2015; Clarke and Warwick, 2001). For the purpose of this study, we set the sim/sd threshold for characterising morphotaxa within and between biotopes to be ≥1.5 (Clarke and Warwick, 2001).

3. Results

3.1. Megafaunal trends on the Schulz Bank

A total of 138 173 individuals were recorded and assigned to 126 morphotaxa (see supplementary materials S4 for complete morphotaxa list), though only a total of 95 morphotaxa with 138 044 individuals were included in the statistical analyses after removal of the rare morphotaxa. Porifera was the dominant phylum in both total density and total number of morphotaxa present, comprising 56.7% of the total density and 51.6% of the total morphotaxa observed. Chordates were the second most dense group (23.4%), but the least rich in morphotaxa (4.2%). Echinoderms made up 10.7% of the total density and 12.6% of the total morphotaxa present. Cnidarians constituted 8.7% of the total density and 18.9% of morphotaxa richness. Both arthropods and molluscs had low density (0.4% and 0.2%, respectively) and morphotaxa richness (both at 6.3%).

3.2. Identification of communities on the Schulz Bank

The linkage tree analysis identified five main clusters (clusters C, K, S, X, and AB) (Figure 2), where the clusters most closely aligned with regions on the seamount (Summit, Upper Slope, Lower Slope, and Base).

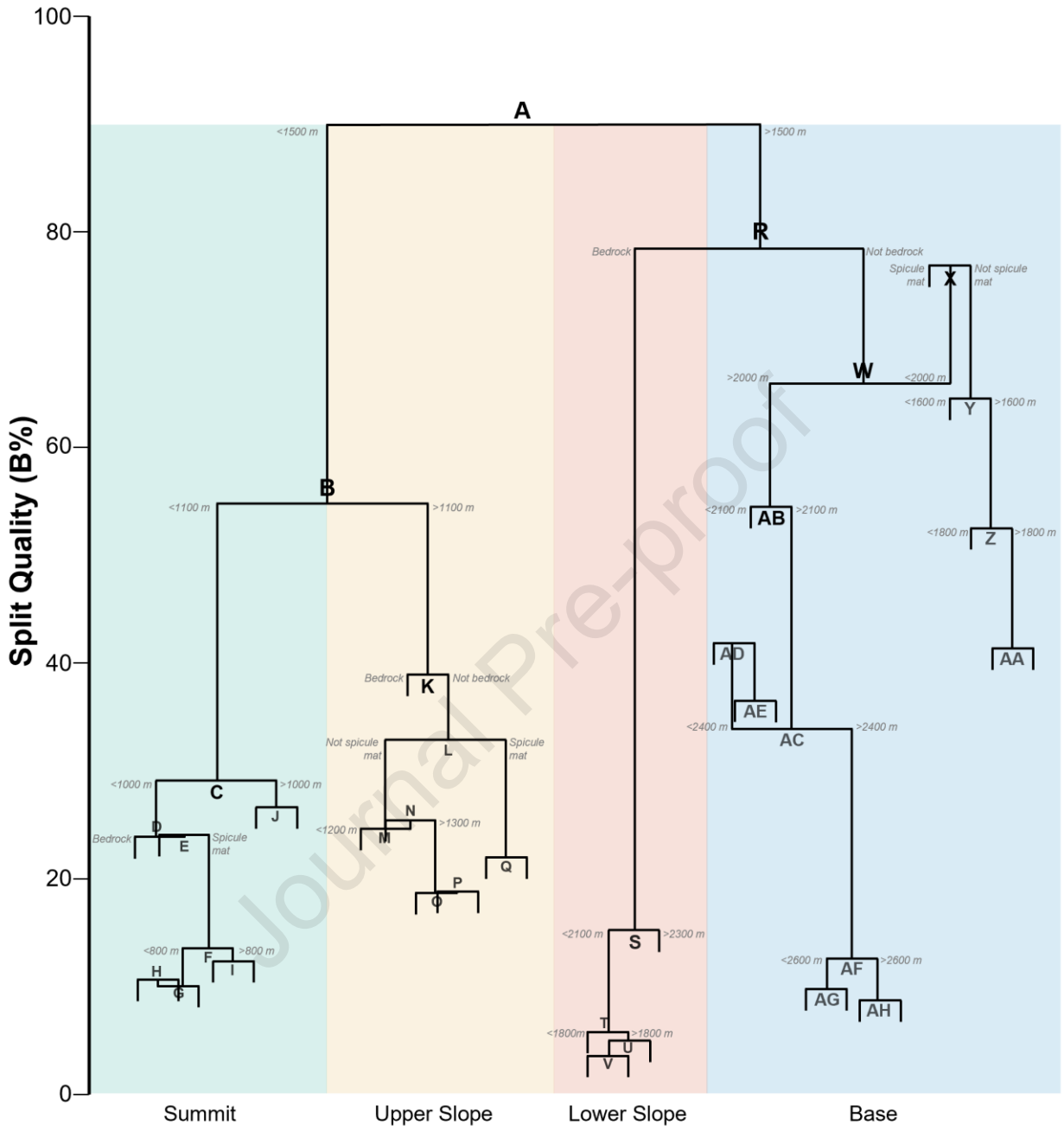

Figure 2. Linkage tree dendrogram of the square-root transformed images reveal the main clusters (C, K, S, X, and AB) from 4 regions on the Schulz Bank based on the split quality (B%): Summit (teal), Upper Slope (yellow), Lower Slope (red), and Base (blue).

The linkage tree was initially split into two main clusters (clusters B and R) at 89.9%, where the splitting was most influenced by depth (above or below 1500 m; R=0.7, sig = 0.0001). The splitting between clusters on the summit and upper slope (clusters C and K) at 54.8% was most influenced by depth interval (above or below 1100 m; R=0.92, sig = 0.0001). Continuing with the clusters on the summit, another split (clusters D and J) occurred at 29.1% and was also

most influenced by depth (above or below 1000 m; R=0.88, sig = 0.0001). The following splits were primarily influenced by substratum type, where cluster E was predominately influenced by spicule mat. In the clusters on the upper slopes, the third (cluster L) and fourth (clusters M and Q) split was influenced by substratum type (bedrock or not bedrock, spicule mat or not spicule mat, respectively). The main splitting between the clusters on the lower slope and base (clusters S and W) at 78.5% were due to substratum type, where the lower slope clusters (cluster S) was most influenced by bedrock. The following splits in the lower slope were due to depth intervals. In the clusters on the base, there was a split (clusters X and AB) at 65.9% due to depth (above or below 2000 m; R =0.55, sig = 0.0001). On cluster X, the initial splitting was due to substratum type (spicule mat or not spicule mat), followed by depth intervals. On cluster AB, the splits were most influenced by depth intervals.

Non-metric Multi-Dimensional Scaling (nMDS) ordination plots showed that the five clusters identified by the linkage tree analysis were generally well separated in the ordination space, where the images within the clusters C and S were grouping most closely together (Figure 3). However, there was some of overlap in the ordination plot between clusters X and AB, and X and S. Similar to what was observed in the linkage tree analysis, there was a split between the shallower clusters (clusters C and K) and the deeper ones (clusters S, X, and AB).

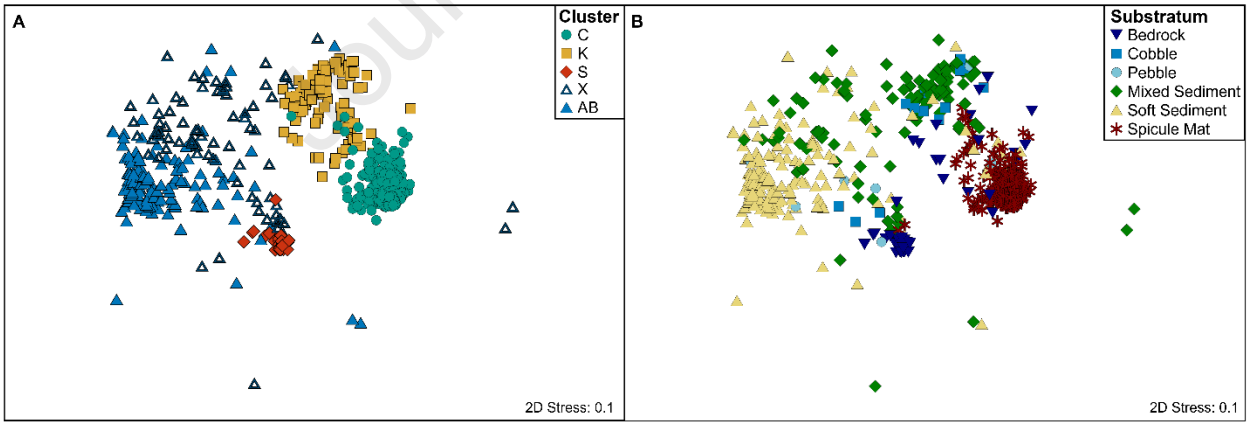

Figure 3. Non-metric Multi-Dimensional Scaling (nMDS) ordination plots of the square-root transformed images on the Schulz Bank. A) Clusters identified in the linkage tree analysis (Figure 2), where color and shape indicates the region the clusters are in: Summit (teal circles), Upper Slope (yellow squares), Lower Slope (red diamonds), and Base (blue triangles, open and filled). B) Dominant substratum superimposed over the datapoints in the ordination space

Superimposing the dominant substrata on the ordination plot showed consistency in the dominant substratum within the biotopes. For cluster C (Summit), spicule mat was the dominating

substratum and was present in 92% of samples in this biotope, with patches of soft sediment (4%), bedrock (3%), and mixed sediment (1%). Cluster K (Upper Slope) was mainly dominated by mixed substratum (60%), followed by spicule mat (15%), cobble (11%), bedrock (11%), soft sediment (2%), and pebble (1%). Cluster S (Lower Slope) was dominated by bedrock (100%). Cluster X (Base) was primarily covered in mixed sediment (53%), followed by soft sediment (42%) spicule mat (4%), and cobble (1%). Cluster AB (Base) was primarily dominated by soft sediment (87%), followed by mixed sediment (8%), pebble (3%), and cobble (1%).

3.3. Community and diversity trends

Cluster C occurred on a continuous spicule mat from ~579–1100 m (Figure 4). It had the second highest average community density (120.88±3.20 ind. m^{-2} (mean±st. error)). The species rarefaction curve approached the asymptote at 75 morphotaxa, which was the highest number of morphotaxa present out of all biotopes. The images in this cluster had an average number of morphotaxa per image of 23.22±0.28.

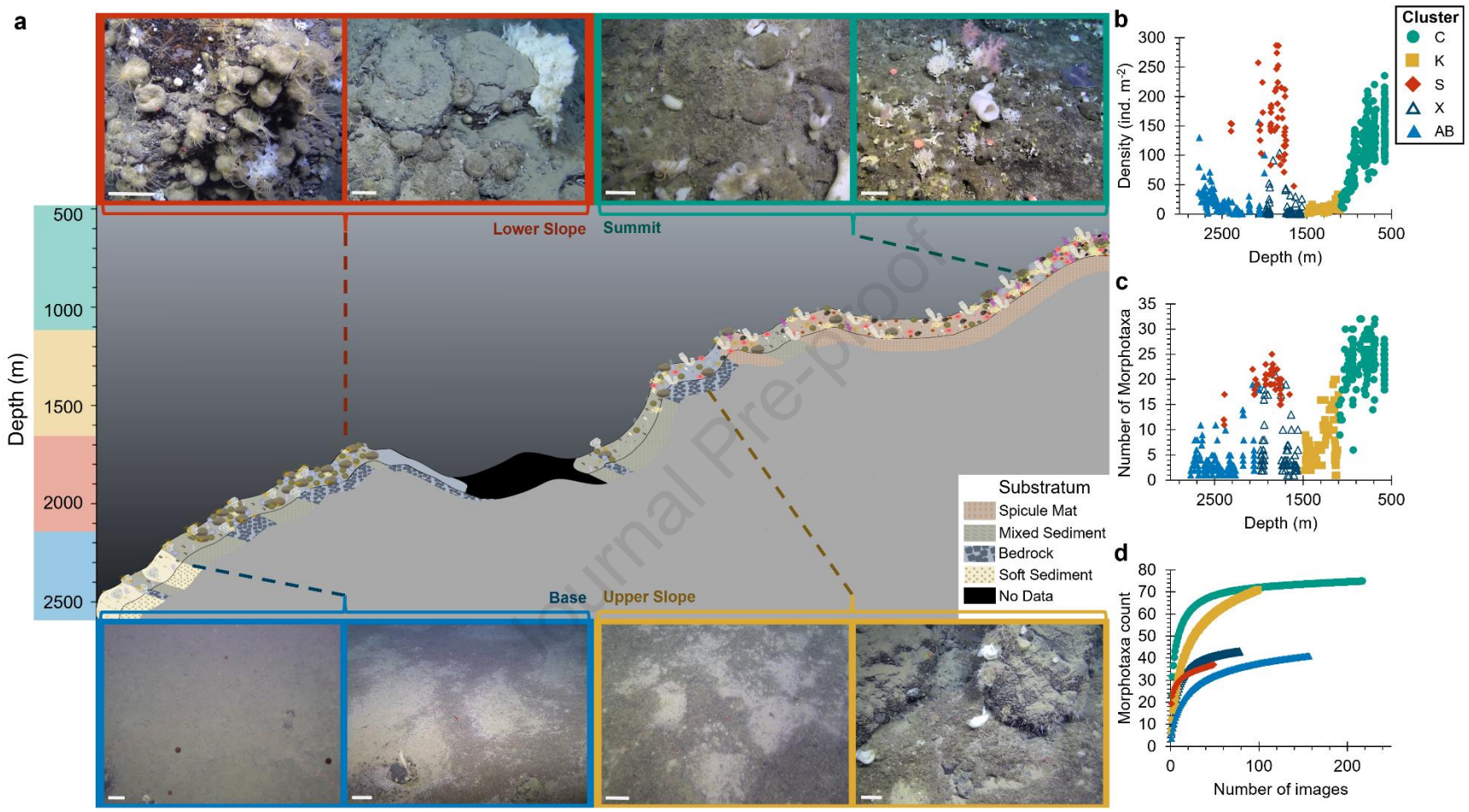

Figure 4. Community distribution and trends on Schulz Bank, Arctic Mid-Ocean Ridge. a) Profile schematic with representative images highlighting the distribution of respective communities and dominant substrata. Expanded schematics and additional image plates of each biotope can be seen in Figures 5 to 7. Morphotaxa size within the schematic is not to scale. Scale bars on image plates are 16 cm long. b–d) Community trends (megafaunal density (b), number of morphotaxa (c), and species accumulation curves (d)) of the images in the respective clusters (Summit (teal circles), Upper Slope (yellow squares), Lower Slope (red diamonds), and Base (blue triangles, open and filled)).

Cluster K occurred from ~1100–1485 m depth and was found primarily on mixed sediment with patches of hard substratum and spicule mat. This cluster had the second lowest average community density compared to the other communities (12.95±0.80 ind. m^{-2}). The total number of morphotaxa throughout this cluster was second highest compared to the other clusters (71 morphotaxa), although the species rarefaction curve did not reach the asymptote. The suggests either the sampling efforts did not fully represent all the morphotaxa in this cluster and could have a higher number of morphotaxa overall, even though the average number of morphotaxa per image is lower than adjacent zones (7.15±0.45). Therefore, this cluster may act as a transitional zone that incorporates the distinct summit taxa (but in lower densities).

The lower slope community (cluster S) formed predominately on bedrock walls from ~1655–2400 m. There was a spike in density that was comparable to what was observed in cluster C, where the average community density was 161.95±8.15 ind. m^{-2}, the highest average density of the five clusters. It had the lowest number of morphotaxa present (37 morphotaxa), although the species rarefaction curve did not fully reach the asymptote. There was an average number morphotaxa per image being 19.37±0.38.

Cluster X occurred primarily on both mixed and soft sedimented areas from ~1555–1980 m. This community had the lowest average community density at 10.09±2.11 ind. m^{-2}. It had 43 morphotaxa identified by the species rarefaction curve, although the curve did not reach the asymptote. The average number of morphotaxa observed per image was 5.68±0.58.

The final cluster, cluster AB, occurred from 2000–2775 m on soft sediment. This cluster had an average community density of 19.01±1.78 ind. m^{-2}. The species rarefaction curve approached an asymptote at 41 morphotaxa. This cluster had the lowest average morphotaxa per image of 3.76±0.27.

3.4. Community description

Cluster C was mainly dominated by sponges (Figure 5), which made up 56.8% of the total morphotaxa density (126.14 ind. m^{-2}). Ascidians were the second most dense group, contributing to 29.6% of the total morphotaxa density, followed by cnidarians (10.5%). Echinoderms (2.8%), arthropods (0.2%), and molluscs (0.1%) were the least dense phyla. In this community, large structure-forming sponges (namely *Schaudinnia rosea* / *Trichasterina borealis* / *Scyphidium septentrionale* 213; *Asconema foliatum* (Fristedt, 1887) 135; *Geodia parva* Hansen, 1885 /

Stelletta rhaphidiophora Hentschel, 1929 211; *Geodia hentscheli* Cárdenas, Rapp, Schander & Tendal, 2010 105) were distributed throughout the area with an average density (± st. error) of 9.15±0.65 ind. m^{-2} (min–max: 0.47–65.27 ind. m^{-2}), with smaller demosponges, ascidians, and cnidarians settled between the large sponges. The branching sponge, *Lissodendoryx (Lissodendoryx) complicata* 114 was densely aggregated throughout the area, with an average clumping density of 17.84±0.79 clumps m^{-2} (min–max: 0.25–80.29 clumps m^{-2}). It was not uncommon to observe *Gersemia rubiformis* (Ehrenberg, 1834) inc. 36 settled directly on the large demosponges or Actinostolidae indet. 24 on top of *Ascidia obliqua* Alder, 1863 inc. 19. Asteroids (*Tylaster willei* Danielssen & Koren, 1881 49) regularly appeared to feed on *G. parva* / *S. rhaphidiophora* 211, and in some cases *S. rosea* / *T. borealis* / *S. septentrionale* 213. *Hexadella dedritifera* Topsent, 1913 110 was frequently observed growing on *G. parva / S. rhaphidiophora* 211. *Isidella* sp. indet. 39 was only observed in this community and found in patches from ~845–1035 m depth (average clumping density: 3.16±0.91 clumps m^{-2} (min–max: 0.85–10.73 clumps m^{-2}). While not included in the analyses, there was a high density of *Amblyraja hyperborea* (Collett, 1879) egg cases (average density: 0.31±0.04 ind. m^{-2}; min–max: 0.05–0.91 ind. m^{-2}) from ~580–760 m depth, which was not seen elsewhere on the seamount.

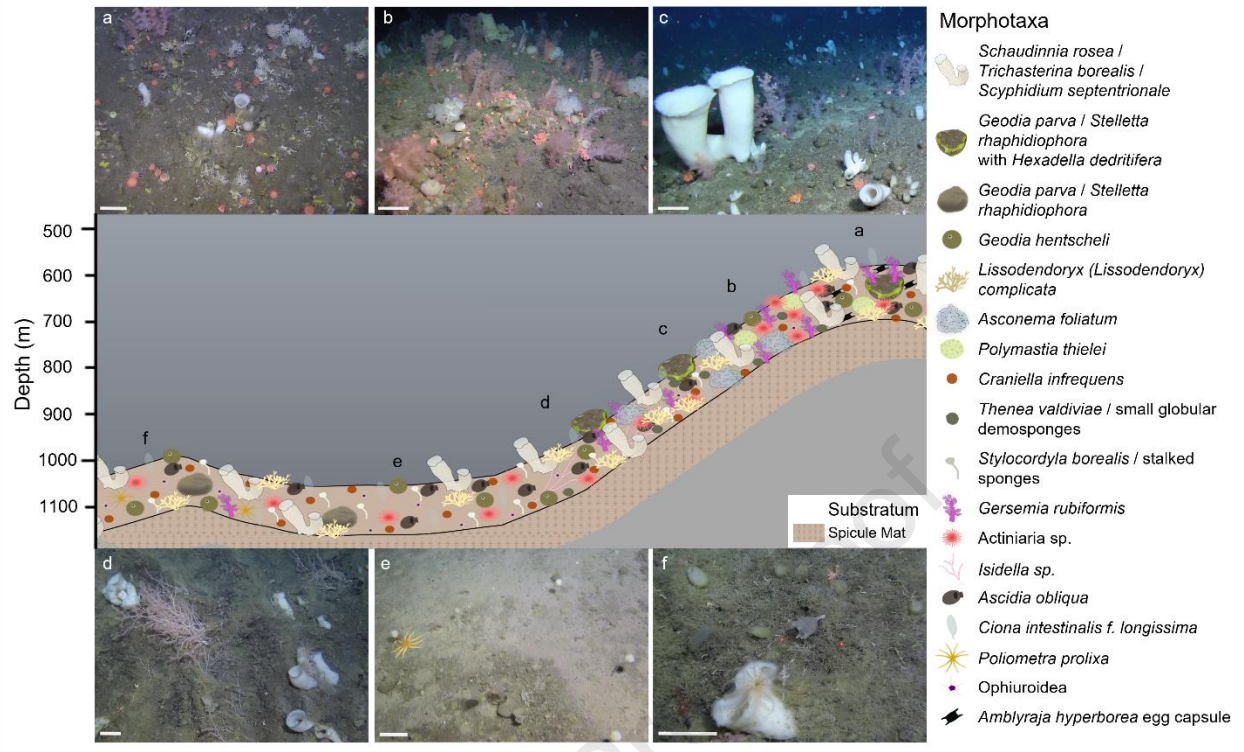

Figure 5. Schematic of cluster C biotope occurring on the summit of the Schulz Bank from 580 to 1100 m depth, where the panels represent changes in community structure with depth. Morphotaxa size within the schematic is not to scale. Scale bars on image plates are 16 cm long.

Cluster K had a high density of echinoderms (66.7% of the total morphotaxa density (12.94 ind. m^{-2}), followed by porifera (15.4%), ascidians (7.4%), cnidarians (6.6%), arthropods (2.4%), and molluscs (1.5%) (Figure 6). The same structure-forming sponges observed in cluster C were present in this biotope in patchy occurrences, with an average density 0.86±0.11 ind. m^{-2} (min–max: 0.19–2.68 ind. m^{-2}). Ophiuroidea indet. 60 was densely aggregated throughout cluster K (average density: 7.92±0.77 ind. m^{-2}; min–max: 0.19–33.10 ind. m^{-2}). The crinoid, *Poliometra prolixa* (Sladen, 1881) 56 (average density: 0.57±0.13 ind. m^{-2}; min – max: 0.23 – 1.76 ind. m^{-2}), was commonly positioned on the rim of the oscula of *S. rosea* / *T. borealis* / *S. septentrionale* 213. The scalpellid, *Catherinum striolatum* (Sars G.O., 1877) 08, was occasionally seen on hard substrata in the deeper region of this cluster (average density: 0.80±0.12 ind. m^{-2} (min–max: 0.23–2.76 ind. m^{-2}). *Neohela* sp. indet. 18 burrows were observed on occasion in this region, though visible individuals were rarely detected (average density: 0.46±0.07 ind. m^{-2}; min–max: 0.25–0.65 ind. m^{-2}).

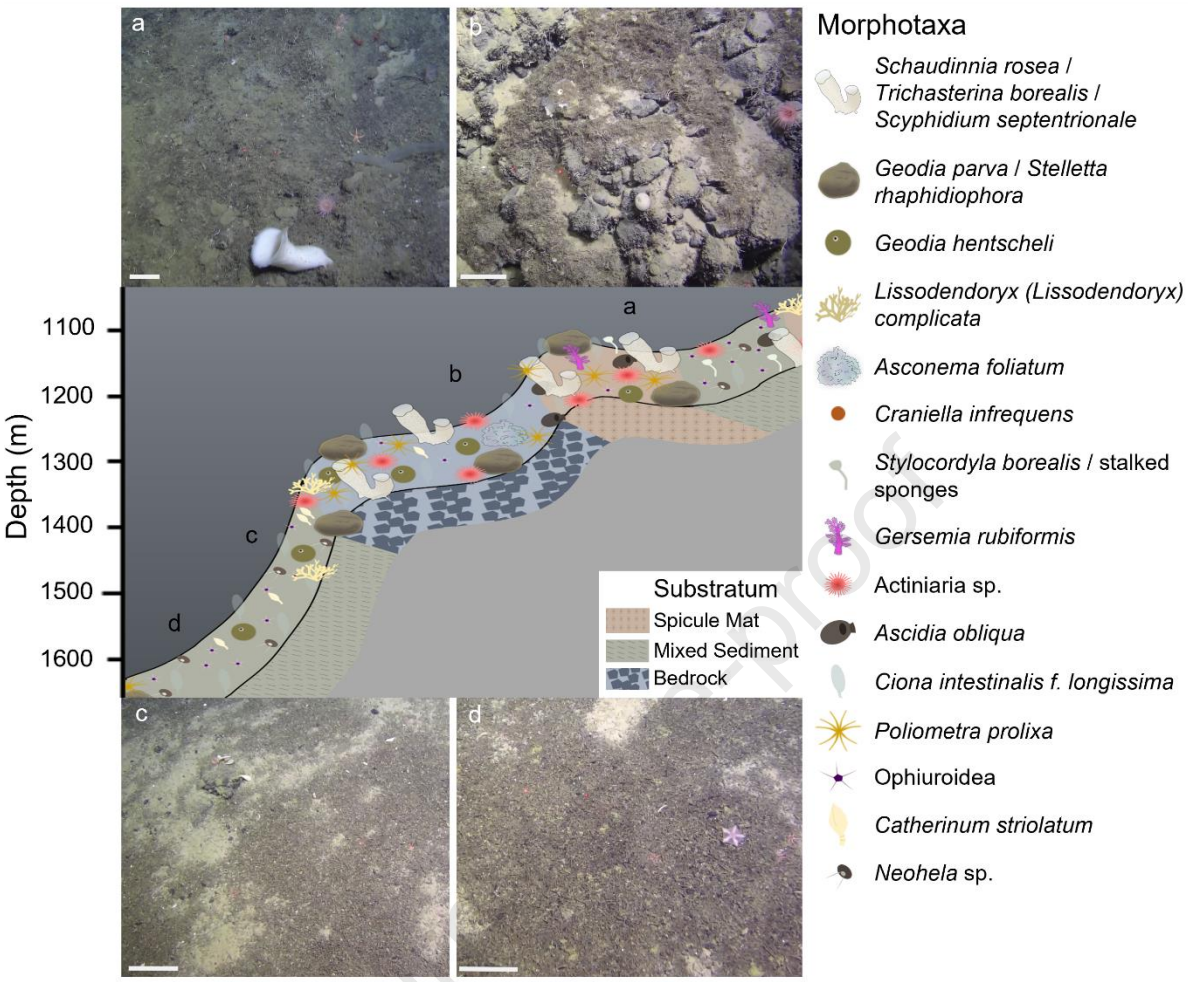

Figure 6. Schematic of the communities in cluster K occurring on the upper slope of Schulz Bank from 1100 to 1600 m depth, where the panels represent changes in community structure with depth. Morphotaxa size within the schematic is not to scale. Scale bars on image plates are 16 cm long.

Cluster S primarily comprised of dense aggregations of sponges on the bedrock walls (Figure 7a), making up 83.9% of the total morphotaxa density (153.05 ind. m^{-2}). Echinoderms were the second densest group (12.9%), followed by ascidians (2.5%), arthropods (0.4%) cnidarians (0.2%), and molluscs (0.02%). The large structure-forming sponges (Aphrocallistidae inc. 144, *G. parva / S. rhaphidiophora* 211, *G. hentscheli* 105, and Axinellidae indet. 95) had an average density of 35.62±2.35 ind. m^{-2} (min–max: 1.87–68.31 ind. m^{-2}). Like in cluster C on the summit, *Lissodendoryx (Lissodendoryx) complicata* inc. 115 was also observed here in dense patches (average clumping density:10.63±0.93 clumps m^{-2}; min–max: 1.80–25.15 clumps m^{-2}). *Poliometra prolixa* 56, was often settled directly on *G. parva / S. rhaphidiophora* 211, Axinellidae indet. 95, or the bedrock walls (average density: 21.65±3.11 ind. m^{-2}; min–max: 1.71–

450 125.54 ind. m^{-2}). The decapod, *Bythocaris leucopis* G. O. Sars, 1879 216, was also commonly seen
451 directly on the large structure-forming sponges.

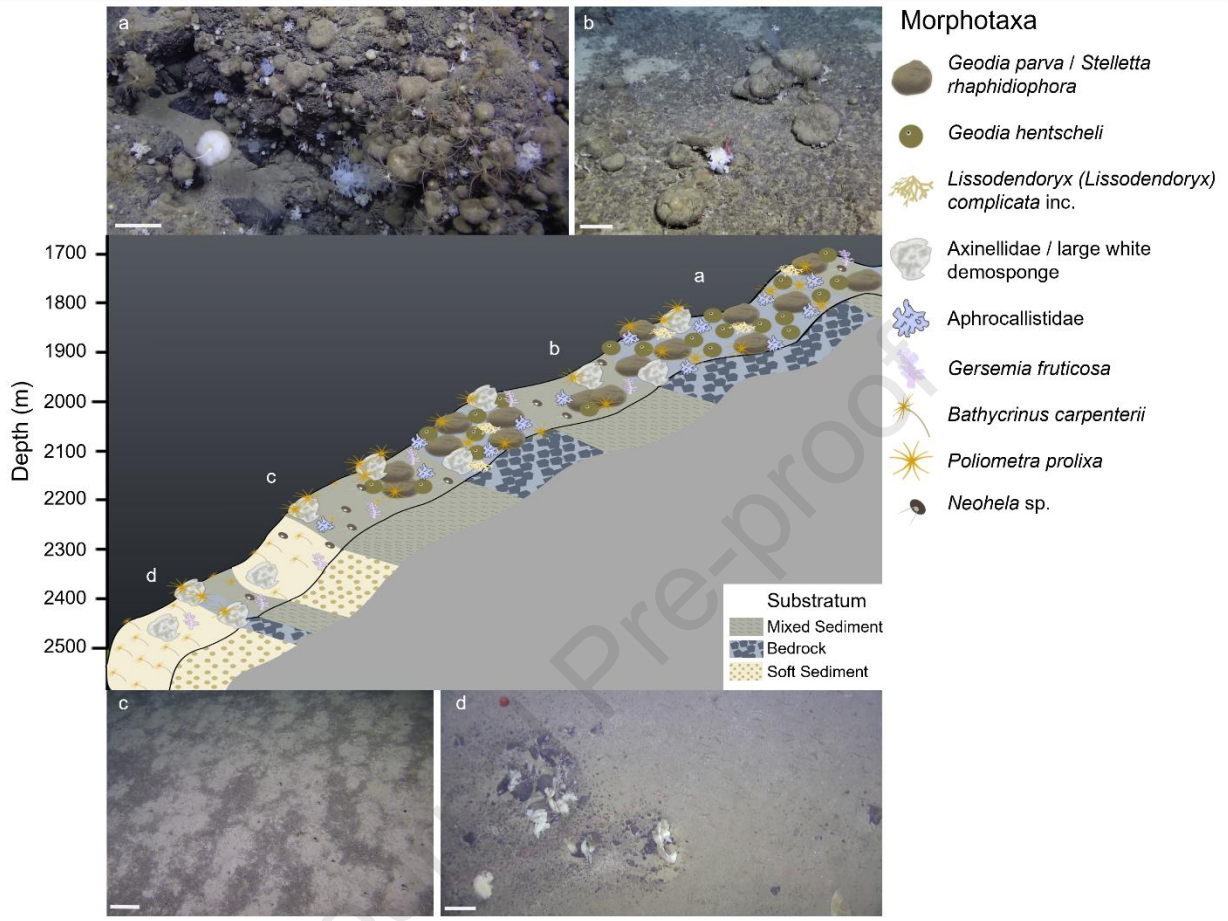

452

453 Figure 7. Schematic of the communities in S, X, and AB clusters occurring on the Schulz Bank from 1555
454 to 2775 m depth, where a) represents cluster S; b–c) symbolizes cluster X; and d) visualizes cluster AB.
455 Morphotaxa size within the schematic is not to scale. Scale bars on image plates are 16 cm long.
456

457 Cluster X (Figure 7b and c) was a relatively sparse group. Here, porifera was the
458 dominating group (67.8% of the total morphotaxa density (9.13 ind. m^{-2})), followed by
459 echinoderms (16.5%), arthropods (7.6%), cnidarians (6.6%), ascidians (1.6%), and molluscs
460 (0.6%). Patches of the same structure-forming sponges found in Cluster S were occasionally
461 observed on mixed sediment (average individual density: 9.25±2.21 ind. m^{-2}; min–max: 0.30–
462 33.85 ind. m^{-2}). *Neohela* sp. indet. 18 burrows were frequently observed here, with a few *Neohela*
463 individuals visible in the video footage (average individual density: 0.95±0.10 ind. m^{-2}; min–max:
464 0.23–2.53 ind. m^{-2}). The stalked crinoid, *Bathycrinus carpenterii* (Danielssen & Koren, 1877) 55,

465 was found intermittently in this region (average individual density: 0.95±0.10 ind. m^{-2}; min–max:
466 0.23–2.53 ind. m^{-2}).

467 Cluster AB (Figure 7d) was most dominated by echinoderms, making up 83.6% of the total
468 morphotaxa density (19.30 ind. m^{-2}), followed by porifera (11.3%), cnidarians (4.1%), arthropods
469 (0.8%), molluscs (0.03%), and ascidians (0.02%). *Bathycrinus carpenterii* 55 dominated the soft
470 bottom regions, with an average density of 16.34±1.48 ind. m^{-2} (min–max: 0.43–129.23 ind. m^{-2}).
471 Large structure-forming sponges were infrequently observed (average density: 1.48±0.32 ind. m^{-2};
472 min–max: 0.23–11.92 ind. m^{-2}), and generally only occurred on the occasional available hard
473 substratum. The hydrozoan, *Crossota* sp. indet. 43, was regularly noted in the water column above
474 the benthos.

475 **3.5. Characteristic taxa**

476 The SIMPER analysis revealed that faunal similarity of the clusters varied (Table 2). On the
477 summit, cluster C had an average within-group similarity of 55.78%. The characterising
478 morphotaxa identified in this cluster were large glass sponges, demosponges, ascidians, and
479 cnidarians. These morphotaxa also consistently contributed most to the similarity within cluster C
480 and dissimilarity between the other clusters. Cluster C was least similar to cluster AB (average
481 similarity = 0.40%).

482

Table 2. Overview of the depth range, dominant substratum, and characterising morphotaxa with their percent contribution in the clusters identified by the linkage tree analysis (Figure 2). Vulnerable Marine Ecosystem (VME) indicator taxa are bolded (ICES, 2020). Characterising morphotaxa are taxa that were determined to consistently contribute most to the similarity (sim/sd ≥ 1.5) within groups and between groups in the SIMPER analyses. Asterisks (*) indicate that similarity within or dissimilarity between groups was <1.5 between one or more groups.

Cluster	Image Area (m^2)	Number of Images	Depth Range (m)	Dominant Substratum	Average Similarity (%)	Characterising morphotaxa within the biotope (with percent contribution)
C	845.11	217	579–1098	Spicule Mat	55.78	***Schaudinnia rosea* / *Trichasterina borealis* / *Scyphidium septentrionale*** 213 (4.12%), Rossellidae indet. 139 (4.61%), ***Lissodendoryx (Lissodendoryx) complicata*** 114 (10.43%), ***Craniella infrequens*** 100 (6.92%), *Hexadella dedritifera* 110 (8.87%), Off-White Encrusting Sponge 164* (5.80%), Off-White Encrusting Sponge 154* (5.18%), *Ascidia obliqua* inc. 19 (11.91%), *Ciona intestinalis f. longissima* 214 (11.77%), Actinostolidae indet. 24* (5.62%)
K	267.32	99	1103–1485	Mixed sediment	35.38	Ophiuroidea indet. 60* (71.14%)
S	115.01	49	1654–2397	Bedrock	70.83	***Geodia parva* / *Stelletta rhaphidiophora*** 211 (7.71%), ***Geodia hentscheli*** 105 (9.50%), ***Lissodendoryx (Lissodendoryx) complicata*** inc. 115 (7.27%), Aphrocallistidae sp. inc. 144 (4.06%), *Hymedesmia* sp. inc. 151 (7.90%), Gray Encrusting Sponge 167* (3.46%), Off-White Sponge 174 (4.04%), Small Globular Demosponge 101 (2.82%), Small Globular Demosponge 124* (2.79%), Small Globular Demosponge 125 (3.91%), Small Globular Demosponge 155 (3.13%), Transparent Encrusting Sponge 169* (3.80%), White Demosponge 212 (12.42%), White Encrusting Sponge 132 (3.15%), White Encrusting Sponge 163 (8.89%), *Poliometra prolixa* 56 (9.38%), *Molgula* sp. indet. 23* (2.89%)
X	244.87	78	1557–1982	Mixed and soft sediment	19.38	No characterizing taxa identified
AB	422.19	157	2001–2774	Soft sediment	41.37	***Bathycrinus carpenterii*** 55 (90.9%)

On the upper slope, cluster K had an average within-group similarity of 35.38%. Here, Ophiuroidea indet. 60 consistently contributed most to the similarity within the cluster and dissimilarity between the other clusters. The community structure in cluster K was least similar to cluster AB (average similarity = 1.40%).

Cluster S had the highest within-group similarity (70.83%) compared to the other clusters. Sponges, crinoids, and an ascidian were identified as the top characterising morphotaxa for this cluster and consistently contributed most to the similarity within and dissimilarity between the

clusters (Table 2). The community structure in cluster S was least similar to cluster K (average similarity = 6.39%).

Cluster X had the lowest within-group similarity (19.38%), and no characterizing taxa were clearly identified in this cluster due to all the morphotaxa having a sim/sd or diss/sd lower than 1.5 in the SIMPER analysis. However, the morphotaxa that had the highest sim/sd was *Neohela* sp. indet. 18 (within-group sim/SD = 0.58, contribution percent = 35.18%). Cluster X was least similar to cluster C (average similarity = 2.20%).

Cluster AB had an average within-group similarity of 41.37%. *Bathycrinus carpenterii* 55 was identified as the characterizing morphotaxa of this cluster and contributed most to the similarity and dissimilarity within and between the clusters.

4. Discussion

This study describes the multiple megabenthic biotopes present on the Schulz Bank, from base to summit. We described the community composition, identified biotopes and approximate depth ranges, dominant substrata, and characterising morphotaxa, and explored trends in biotope species richness. Three of the biotopes identified in the present study were characterised by VME indicator taxa (ICES, 2020), although all biotopes contained at least one VME indicator taxa. This study establishes a baseline understanding of the communities on the Schulz Bank, which may share characteristics with other megabenthic communities on the Arctic Mid-Ocean Ridge.

4.1. Arctic biotopes

4.1.1. Arctic sponge grounds on biogenic substratum

In general, similar types of sponge grounds to those observed on the Schulz Bank summit have been reported throughout the Arctic, from north of Spitzbergen in the Central Arctic Ocean to the East Greenland Shelf and in Davis Strait and the Canadian Arctic (Burton, 1934; Klitgaard and Tendal, 2004; Mayer and Piepenburg, 1996; Morganti et al., 2022; Murillo et al., 2018; Unger Moreno et al., 2021). While seamount studies in the Arctic are limited (Clark et al., 2021), the Vesteris Bank (73°30’N 9°10’W) communities contain many of the same taxa and community patterns observed on Schulz Bank (Henrich et al., 1992; Unger Moreno et al., 2021). Vesteris Bank (also referred to as Vesterisbanken Seamount or Vesteris Seamount), is an underwater volcano located in the central Greenland Sea off the eastern coast of Greenland and about 400 km west of

Mohn Ridge on AMOR (Cherkis et al., 1994; Henrich et al., 1992; Mertz and Renne, 1995; Unger Moreno et al., 2021). Like Schulz Bank, Vesteris Bank has a large depth gradient, although with a shallower summit at ~133 m depth and the base at ~3100 m. Based on reports from Henrich et al. (1992) and Unger Moreno et al. (2021), the summit of the seamount is covered in a spicule mat with large sponges (*Geodia, Stelletta*, and *Schaudinnia*), ascidians, cnidarians, and echinoderms dominating the area. The shallower regions of Schulz Bank upper slope, from ~1100 to 1265 m, appears to be a transition zone. There were patches of spicule mat covered in the characteristic summit fauna before transitioning to patches of exposed bedrock with occasional sponges, cnidarians, crinoids, and ascidians. These exposed bedrock communities resembled the pillow lava communities on the deeper slopes of Vesteris Bank (750 to 1075 m depth), where sponges (demosponges and *Schaudinnia*) and crinoids settled (Henrich et al., 1992; Unger Moreno et al., 2021).

Further north in the Central Arctic Ocean, a more recent study by Morganti et al. (2022) found dense sponge grounds (7 to 11 ind. m^{-2}; mean sponge density ± st. deviation: 2.8±1.1 ind. m^{-2}) characterised by *G. parva*, *G. hentscheli*, and *S. rhaphidiophora* on the summits (585 to 721 m) of three extinct volcanos (ridge end points: 87°N 62°E to 85°55’ N 57°45’ E) on Langseth Ridge (AMOR). Like the summit of Schulz Bank, the area is covered in a dense spicule mat (~15 cm thick) and the communities extend from ~580 to 1000 m depth. The sponge ground communities described by Morganti et al. (2022) differ from the Schulz Bank summit communities in that glass and calcareous sponges were observed in low densities, and the associated megafauna consisted of bryozoans, crustaceans, echinoderms, fish, and soft corals. It is interesting to note that for both the summit sponge grounds in the present study and in Morganti et al. (2022), soft corals were documented growing on top of the large demosponges and seastars were observed predating on the sponges as well.

4.1.2. Arctic sponge grounds on hard substratum

One of the most notable observations from this study were the dense aggregations of large demosponges on the bedrock walls on the lower slopes. One noteworthy aspect of this biotope was the high megafaunal density and diversity that were comparable to the shallower summit sponge ground, when seamount summits are generally assumed to have the highest density and species richness compared to the communities on the slopes and base (Bridges et al., 2021; Samadi et al.,

2007, 2006). In addition, the average density for the large structure-forming sponges was comparable to that observed on the summit. However, while not measured in this study, the size of the structure-forming sponges on the summit appears larger than the sponges on the bedrock walls. Therefore, it is likely that the biomass of the structure-forming sponges is higher at the summit, though further investigation is needed.

These geodiid-dominated walls of Schulz Bank resemble similar communities observed around Mohn's Treasure (73°44'N 7°27'E), an inactive sulphide mound on AMOR just south of the Schulz Bank (Ramirez-Llodra et al., 2020), and on the Ægir Ridge System (Brix et al., 2022), a rift valley with a canyon-like structure extending from 700 m to 3800 m depth. On Mohn's Treasure, the bedrock walls were dominated by similar sponges (with a density of 22.4 ind. m^{-2}), crinoids and decapods to those observed on Schulz Bank (Ramirez-Llodra et al., 2020). On Ægir Ridge, geodiid-dominated communities covered the steeply sloping area of the ridge, where consolidated sediment layers were present (Brix et al., 2022). It is interesting to note that the main structure-forming demosponge taxa found on the lower slopes of Schulz Bank, Mohn's Treasure, and Ægir Ridge are the same that form the summit sponge grounds found on seamounts in the Central Arctic Ocean (Morganti et al., 2022). While the Schulz Bank geodiid-dominated communities formed primarily on the bedrock walls, there were patches of geodiid-dominated communities on the more gently sloping lower regions that resembled the communities described by Morganti et al. (2022).

Previous studies assumed that the summit sponge ground was the most dense and diverse community on Schulz Bank (Hanz et al., 2021; Meyer et al., 2019; Morrison et al., 2020; Roberts et al., 2018). However, the geodiid-dominated walls on the lower slope challenge this assumption. Rock walls, vertical cliffs, and steeper regions on seamounts are often overlooked or inaccessible in seamount studies (Bridges et al., 2021; Clark et al., 2010; Morganti et al., 2022; Sánchez et al., 2008), which could lead to missing important communities in the deep-sea.

4.1.3. Ophiuroid beds on mixed sediment

Below 1265 m on the Schulz Bank, communities transitioned to dense ophiuroid beds on mixed sediment, with the presence of the scalpellid, *Catherinum striolatum*, on the occasional rocky outcrops or drop stones. These ophiuroid beds are common on arctic shelves and slopes (Piepenburg and Schmid, 1996; Sswat et al., 2015), and in some locations ophiuroid densities can

591 reach >100 ind. m^{-2} (Piepenburg, 2005). *Catherinum striolatum* is considered an arctic abyssal
592 species that occurs in temperatures and depths below 0°C and 1500 m (Buhl-Mortensen and
593 Hassel, 2021; Nilsson-Cantell, 1978), and in the present study, the scalpellid was found from
594 ~1100 to 2000 m depth and in negative temperatures (Roberts et al., 2018).
595
596 **4.1.4. Stalked crinoid fields on soft bottom**
597 Schulz Bank base communities were similar to a deep-water rocky reef community in the Eastern
598 Fram Strait and base communities on Vesteris Bank and Mohn's Treasure (Henrich et al., 1992;
599 Meyer et al., 2014; Ramirez-Llodra et al., 2020), where *Bathycrinus carpenterii* dominated these
600 base soft bottom regions. Similar to Ramirez-Llodra et al. (2020), the low biodiversity indices
601 were likely a result of the dominance of a single species (i.e., *B. carpenterii*). Dense stalked crinoid
602 fields have been previously noted to occur around the bathyal zones of seamounts (Rogacheva et
603 al., 2013; Samadi et al., 2007), from depths of 460–3800 m in the Arctic Ocean (Rogacheva et al.,
604 2013).
605
606 **4.1.5. *Neohela* communities on mixed sediment**
607 While the amphipod *Neohela* was not determined to be a characterising taxon in the SIMPER
608 analyses, there were high densities of *Neohela* burrows present throughout mixed sediment or soft
609 bottom regions of the upper slopes to the base, most notably in cluster X. *Neohela monstrosa*
610 (Boeck, 1861) has been documented to co-occur with the sea pen *Umbellula encrinus* (Linnaeus,
611 1758) in highly localized patches (10-35 ind. m^{-2}) from depths of 700-1000 m (Buhl-Mortensen et
612 al., 2016, 2020). *Umbellula* was not documented in the videos used for this study; however, the
613 sea pen was observed by Morrison et al. (2020) on the western slopes of Schulz Bank (average
614 depth 1464 m) and in video footage collected on the eastern slopes with high densities of *Neohela*
615 burrows present (pers. obs). Because burrow counts were not included in the present study, the
616 true densities of *Neohela* on the Schulz Bank remain uncertain.
617
618 **4.2. Biotope classification**
619 The present study revealed different biotopes residing on Schulz Bank; however, none of the
620 biotopes observed fits within the current EUNIS classification scheme. The current EUNIS
621 classifications for geodiid-dominated sponge grounds are broad and group all geodiid sponge

grounds occurring in the Atlantic and Arctic together into two classifications (Parry et al., 2015; JNCC, 2015; EUNIS 2019) with the current description that they both are boreal osturs. The only difference made in the two classifications is whether they occur on coarse (EUNIS code: ME3241) or mixed sediment (EUNIS code: ME4221) in the upper bathyal zone (EUNIS, 2019). While this is due to the limited information on sponge grounds as a whole, the generalized classifications for geodiid-dominated grounds contrasts to the classification(s) made for communities of the glass sponge, *Pheronema carpenteri* (Thomson, 1869). *Pheronema carpenteri* form dense sponge grounds (up to 1.53 ind. m^{-2}) on muddy seafloor from approximately 650–1550 m depth along the Mid-Atlantic Ridge (Howell et al., 2016; Maldonado et al., 2016; Rice et al., 1990; Ross and Howell, 2013). Previously, all *P. carpenteri* grounds were classified as one habitat type known as "Facies with *Pheronema grayi*" (EUNIS code: A6.621) (Davies and Moss, 2004). However, the *P. carpenteri* classifications have expanded in recent years to form three separate classifications. These are based on the communities occurring on lower bathyal mud in the Atlantic (EUNIS code: MF6221), upper bathyal mud in the Atlantic (EUNIS code: MF6231), or Mediterranean (EUNIS code: ME6514) (JNCC, 2015; EUNIS, 2019), where the associated taxa differ with depth.

To make up the current knowledge gap, the present study proposes at least four distinct biotopes on the Schulz Bank, where the full proposed EUNIS biotope descriptions can be seen in the supplementary materials (S5). In summary, the first biotope is the summit sponge ground dominated by rossellid sponges and large demosponges with associated filter- and suspension-feeding taxa and fish located on a dense spicule mat. This biotope would most likely have a broad community classification of "Sponge aggregation on Arctic upper bathyal biogenic habitat". The second biotope is the geodiid and crinoid dominated bedrock walls with associated sponges and decapods and would be classified as "Sponge aggregation on Arctic lower bathyal rock". Alternatively, the dense crinoid communities on the sponges resemble the "Sparse communities on Arctic upper bathyal rock" (EUNIS code: ME111) (JNCC, 2015; EUNIS, 2019), and could be included as a separate biotope overlapping the sponge ground biotope. The third biotope is the dense ophiuroid beds on mixed or coarse sediment and most closely resembles "Sparse communities on Atlantic lower bathyal mixed sediment" (EUNIS code: MF421) (JNCC, 2015; EUNIS, 2019), however adjustments would be needed as it is found in the Arctic and in the upper bathyal zone. The fourth main biotope is the stalked crinoid fields on lower bathyal or abyssal muddy sediment, which does not fit within any EUNIS classifications to date (JNCC, 2015;

EUNIS, 2019). In addition to the four distinct biotopes, an additional possible biotope was noted – the *Neohela* communities with *Umbellula* sp. – which most closely resembles the "Seapens and burrowing megafauna on Atlantic Upper bathyal mud" (EUNIS code: ME622) (JNCC, 2015; EUNIS, 2019).

4.3. Drivers of community patterns

While the drivers of community patterns were not examined in this study, it is likely that environmental variables are influencing the biotope distribution based on the trends observed with depth and changes in substrata. Depth itself is not a driver of community patterns and acts as proxy for other parameters (e.g., water mass structure, seafloor characteristics, etc.) (McArthur et al., 2010). Therefore, examining abiotic variables (other than depth and/or latitude and longitude) is needed in order to identify the drivers of species distribution and community structure.

Water mass characteristics have long been hypothesized to be driving sponge ground distribution (Klitgaard and Tendal, 2004), and the different sponge fauna are thought to occur around specific water masses. Several studies have found arctic sponge ground indicator species to be influenced by or broadly associated with water mass properties (e.g., temperature and salinity) of Arctic Intermediate Water or deeper arctic origin water masses (Buhl-Mortensen et al., 2020; Burgos et al., 2020; Murillo et al., 2018; Roberts et al., 2021). Similar findings were observed for other biotopes found in the Arctic (Buhl-Mortensen et al., 2020). While the reason for their association is unclear, it has been suggested that the sponges tolerate a range of water mass properties and variability to benefit from physical and biogeochemical mechanisms linked to water mass structure (e.g., enhanced currents, food supply, larval dispersal, etc.) (Buhl-Mortensen et al., 2020; Roberts et al., 2021).

The near-bottom current speed and internal wave activity are also suspected to influence the distribution of sponge grounds (Davison et al., 2019; Hanz et al., 2021; Klitgaard and Tendal, 2004; Roberts et al., 2018). Studies have documented the presence of internal waves with elevated currents at the summit (Hanz et al., 2021; Roberts et al., 2018), where the internal waves are thought to enhance food supply for the sponges. The steep bedrock walls on the lower slopes also likely have locally enhanced currents which then leads to increased food supply, low sedimentation, and high incidence of hard substrata (Clark et al., 2010; Davies et al., 2009; Meyer et al., 2020, 2014). In addition, increased habitat heterogeneity (through biogenic structures and

substratum) can cause accelerated currents or give access to elevated positions within the benthic boundary layer that can be advantageous to filter-feeding taxa (Buhl-Mortensen et al., 2012; Clark et al., 2010; Riisgård, 2015), resulting in high faunal diversity. Areas with slow bottom currents, such as the soft-sedimented base, may have high sedimentation rates that allow for organic matter to settle on the seafloor, possibly acting as an important food source for *B. carpenterii* (Meyer et al., 2014). All these factors could explain the distribution of biotopes and community trends observed; however, investigation of the abiotic drivers is needed in future studies as this was beyond to scope of the current study.

4.4. Limitations

It is likely that the data underrepresents the megabenthic community structure either in terms of density or species richness, as is common with studies that only use video or image annotation to describe communities (Durden et al., 2016; Meyer et al., 2019; Sánchez et al., 2009; Schoening et al., 2012). For example, morphotaxa present in localised patches, rare occurrences, or with a body size smaller than 1 cm may have been missed by the transecting nature of our visual surveys. This study solely describes the general trends in habitat and biotope structure observed in the annotated video footage, therefore the reported depth ranges for the species' occurrences may not be exact. While this study primarily incorporates video footage from the western side of the seamount (particularly in the deeper regions), the biotopes described here are qualitatively consistent with what was noted in other studies on Schulz Bank (Morrison et al., 2020; Roberts et al., 2018) and observed in other transects on the eastern slopes (supplementary materials S6). Those transects were not included in this study due to the inconsistent use of lasers throughout the transects, where lasers were not on in most of the footage.

4.5. Implications for conservation

Deep-sea mining may become a future threat to benthic communities on AMOR, and deep-sea sponges are especially vulnerable due to their slow growth and risk of smothering (Hogg et al., 2010). While locations such as Schulz Bank or Loki's Castle are likely not going to be direct targets of mining, other vent fields containing seafloor massive sulphide deposits or seamounts hosting manganese crusts in the vicinity may be (Olsen et al., 2016; Ramirez-Llodra et al., 2020). Currently, not much is known about the effect deep-sea mining will have on nearby benthic

communities, but it may have similar impacts to deep-sea bottom fishing (Clark et al., 2010). This is due to the risks of habitat loss caused during mining operations or potential toxicity and smothering from sedimentation of the mining plumes (Miller et al., 2018; Vad et al., 2021; Washburn et al., 2019; Wurz et al., 2021). Mining sites focusing on seafloor massive deposits or manganese crusts could lead to transport of sediment plumes to adjacent communities and result in adverse effects for the filter feeding taxa, which needs to be considered when planning such operations (Boschen et al., 2013; Dunn et al., 2018; Miller et al., 2018; Ramiro-Sánchez et al., 2019).

To the best of our knowledge, there is only one marine protected area and nature reserve on AMOR at Jan Mayen (70°59'N 8°32'W) and it covers a total area of 4318.6 km^2 (Marine Protection Atlas, accessed 12 January 2022). This area is currently at a level of "Less Protected" where it has some protection but moderate to extensive extraction (by fisheries) is allowed. Given the rich communities, some of which classify as VMEs (e.g., sponge aggregations and stalked crinoid aggregations; ICES, 2020) on its summit, slopes, and base, the Schulz Bank would be a prime candidate area for designation as an Ecologically and Biologically Significant Area (EBSA) and the establishment of a marine protected area. The relatively pristine condition (e.g., limited anthropogenic disturbances to date) of the community structure would also make the location suitable for an observatory for studying arctic deep-sea sponge grounds in the future (and any impacts that may arise).

The results from this study lay the foundation for future sponge ground modeling studies by forming a baseline understanding of the different biotopes on Schulz Bank, their depth range, and the dominant substrate they occur on. Abiotic variables besides depth and dominant substratum were not considered for this study, but future studies intend to examine the relationship between the abiotic variables and the trends observed with the structure-forming sponge taxa and biotopes on Schulz Bank. While habitat mapping and species distribution modeling studies of sponge grounds or sponge ground forming taxa have become more common in recent years (Beazley et al., 2021, 2018, 2015; Burgos et al., 2020; Chu et al., 2019; Howell et al., 2016; Knudby et al., 2013; Liu et al., 2021), knowledge on the ecology and habitat requirements for some sponge grounds is still being expanded upon, especially for arctic communities. By grouping together multiple sponge species of the same genus that have different environmental thresholds (e.g., boreal, temperate, arctic species) (Howell et al., 2016; Knudby et al., 2013) or including

limited datasets in the model (Liu et al., 2021), the model outputs are based upon broad assumptions and might not reflect the true environmental drivers required for the specific type of sponge ground. Therefore, baseline studies like the present study are crucial for expanding the knowledge of sponge ground ecology and habitat preferences. The results from this study can contribute to improving the accuracy of species distribution models and mapping efforts in the future.

4.6. Conclusion

This study revealed a benthic community (i.e., arctic sponge aggregations on bedrock walls) with densities and diversities that are comparable to the sponge ground on the summit of Schulz Bank. In addition, other communities (e.g., stalked crinoid fields, ophiuroid beds, *Neohela* communities, etc.) were described which further extended our view beyond the arctic sponge ground on the summit. This study improves the current understanding of the summit sponge ground extent, identifies the variation of species composition across the biotopes, and contributes to new descriptions of arctic biotopes for habitat classification systems, such as EUNIS.

Schulz Bank hosts diverse megabenthic communities that contain VME indicator species, and as such, represents a prime candidate for a marine protection area on the Arctic Mid-Ocean Ridge. This location can serve as an observation site for studying arctic sponge ground ecology and surveying the impacts of anthropogenic disturbances in the future. While abiotic drivers were not examined in the present study, the changes in species composition and diversity are likely influenced by them and we aim to examine those drivers in upcoming work. The results presented in this study provide a baseline understanding of the communities on Schulz Bank and lay the foundation for future investigative studies.

Data availability statement

The dataset presented in this article is available at https://doi.pangaea.de/10.1594/PANGAEA.949920.

Declaration of competing interest

None to declare.

Acknowledgements

The work leading to this publication has received funding from the European Union's Horizon 2020 research and innovation programme through the SponGES project (grant agreement No 679849). This publication reflects only the authors' view and the Executive Agency for Small and Medium-sized Enterprises (EASME) is not responsible for any use that may be made of the information it contains. JX research is further supported by national funds through FCT Foundation for Science and Technology within the scope of UIDB/04423/2020, UIDP/04423/2020, and CEECIND/00577/2018. PAR was further supported by the Research Council of Norway (project no. 326881). We would like to thank the University of Bergen, crew of the R.V. *G.O. Sars*, and the pilots of ROV *Ægir6000* for their hard work and making the collection of the video footage and material possible. We would like to offer our most sincere gratitude towards the taxonomists, technicians, and experts who helped confirm the identifications of the taxa from the imagery data - Mari Heggernes Eilertsen, Tone Ulvatn, and Anne Helene Tandberg for aiding with the megafauna identifications; Kenneth Meland for looking over the mysids; Paco Cárdenas, Pilar Rios, Javier Cristobo, and Jon Hestetun for helping identify the sponges; Heather Glon, Meg Daly, and Declan Morrissey for the help of identifying the cnidarians; Bjørn Gulliksen for identifying the tunicates; Nicolas Straube and Ingvar Byrkjedal for identifying the fish on the Schulz; and David Rees for barcoding some of the associated taxa. Additional thanks are offered to Ulrike Hanz and Furu Mienis for expanding more on the oceanographic setting of Schulz Bank. This publication is dedicated to Hans Tore Rapp for his love and expertise of sponges and exploration of the Schulz Bank. Without you, none of this would be possible and we miss you every day.

Author CRediT contributions

H.K. Meyer: Conceptualization, Formal analysis, Investigation, Methodology (video acquisition, video annotation, data acquisition, data preparation, fauna identification, statistics), Visualization, Writing – original draft, Writing – review and editing. ***A.J. Davies:*** Conceptualization, Data curation, Investigation, Methodology (data acquisition, data preparation, and statistics), Resources, Software, Writing – original draft, Writing – review and editing. ***E.M. Roberts:*** Conceptualization, Investigation, Methodology (video acquisition), Writing – original draft,

Writing – review and editing. ***J.R. Xavier:*** Conceptualization, Funding acquisition, Investigation, Methodology (fauna identification; statistics), Project administration, Resources, Writing – original draft, Writing – review and editing. ***P.A. Ribeiro:*** Investigation, Writing – original draft, Writing – review and editing. ***H. Glenner:*** Methodology (fauna identification), Writing – original draft. ***S.-R. Birkeley:*** Methodology (fauna identification), Writing – review and editing. ***H.T. Rapp:*** Conceptualization, Funding acquisition, Investigation, Methodology (video acquisition, fauna identification), Resources, Supervision, Project administration.

References

Baco, A.R., 2007. Exploration for Deep-Sea Corals on North Pacific seamounts and Islands. Oceanography 20, 108–117. https://doi.org/10.5670/oceanog.2007.11

Beazley, L., Kenchington, E., Murillo, F.J., Brickman, D., Wang, Z., Davies, A.J., Roberts, E.M., Rapp, H.T., 2021. Climate change winner in the deep sea? Predicting the impacts of climate change on the distribution of the glass sponge *Vazella pourtalesii*. Mar. Ecol. Prog. Ser. 657, 1–23. https://doi.org/10.3354/meps13566

Beazley, L., Kenchington, E., Yashayaev, I., Murillo, F.J., 2015. Drivers of epibenthic megafaunal composition in the sponge grounds of the Sackville Spur, northwest Atlantic. Deep. Res. Part I Oceanogr. Res. Pap. 98, 102–114. https://doi.org/10.1016/j.dsr.2014.11.016

Beazley, L., Wang, Z., Kenchington, E., Yashayaev, I., Rapp, H.T., Xavier, J.R., Murillo, F.J., Fenton, D., Fuller, S., 2018. Predicted distribution of the glass sponge *Vazella pourtalesi* on the Scotian Shelf and its persistence in the face of climatic variability. PLoS One 13, 1–29. https://doi.org/10.1371/journal.pone.0205505

Boschen, R.E., Rowden, A.A., Clark, M.R., Gardner, J.P.A., 2013. Mining of deep-sea seafloor massive sulfides: A review of the deposits, their benthic communities, impacts from mining, regulatory frameworks and management strategies. Ocean Coast. Manag. 84, 54–67. https://doi.org/10.1016/j.ocecoaman.2013.07.005

Bowering, W.R., Nedreaas, K.H., 2000. A comparison of Greenland halibut (*Reinhardtius hippoglossoides* (Walbaum)) fisheries and distribution in the Northwest and Northeast Atlantic. Sarsia 85, 61–76. https://doi.org/10.1080/00364827.2000.10414555

Bridges, A.E.H., Barnes, D.K.A., Bell, J.B., Ross, R.E., Howell, K.L., 2021. Benthic Assemblage Composition of South Atlantic Seamounts. Front. Mar. Sci. 8, 1–18.

https://doi.org/10.3389/fmars.2021.660648

Brix, S., Kaiser, S., Lörz, A., Le Saout, M., Schumacher, M., Bonk, F., Egilsdóttir, H., Olafsdottir, S.H., Tandberg, A.H.S., Taylor, J., Tewes, S., Xavier, J.R., Linse, K., 2022. Habitat variability and faunal zonation at the Ægir Ridge , a canyon-like structure in the deep Norwegian Sea. PeerJ 10:e13394. https://doi.org/https://doi.org/10.7717/peerj.13394

Buhl-Mortensen, L., Buhl-Mortensen, P., Dolan, M.F.J.J., Dannheim, J., Bellec, V., Holte, B., 2012. Habitat complexity and bottom fauna composition at different scales on the continental shelf and slope of northern Norway. Hydrobiologia 685, 191–219. https://doi.org/10.1007/s10750-011-0988-6

Buhl-Mortensen, L., Hassel, A., 2021. Distribution and habitat of Scalpellidae (Cirripedia: Thoracica) in the Norwegian and Barents Seas. Mar. Biol. Res. 17, 223–233. https://doi.org/10.1080/17451000.2021.1928220

Buhl-Mortensen, L., Tandberg, A.H.S., Buhl-Mortensen, P., Gates, A.R., 2016. Behaviour and habitat of *Neohela monstrosa* (Boeck, 1861) (Amphipoda: Corophiida) in Norwegian Sea deep water. J. Nat. Hist. 50, 323–337. https://doi.org/10.1080/00222933.2015.1062152

Buhl-Mortensen, P., Dolan, M.F.J., Ross, R.E., Gonzalez-Mirelis, G., Buhl-Mortensen, L., Bjarnadóttir, L.R., Albretsen, J., 2020. Classification and mapping of benthic biotopes in Arctic and Sub-Arctic Norwegian Waters. Front. Mar. Sci. 7, 1–15. https://doi.org/10.3389/fmars.2020.00271

Burgos, J.M., Buhl-Mortensen, L., Buhl-Mortensen, P., Ólafsdóttir, S.H., Steingrund, P., Ragnarsson, S., Skagseth, Ø., 2020. Predicting the distribution of indicator taxa of vulnerable marine ecosystems in the Arctic and Sub-arctic Waters of the Nordic Seas. Front. Mar. Sci. 7, 1–25. https://doi.org/10.3389/fmars.2020.00131

Burton, M., 1934. Report on the sponges of the Norwegian expeditions to East Greenland 1930, 1931, and 1932. Skrifter om Svalbard og Ishavet, 61, 1-33.

Busch, K., Hanz, U., Mienis, F., Mueller, B., Franke, A., Roberts, E.M., Rapp, H.T., Hentschel, U., 2020. On giant shoulders: How a seamount affects the microbial community composition of seawater and sponges. Biogeosciences 17, 3471–3486. https://doi.org/10.5194/bg-17-3471-2020

Cárdenas, P., Rapp, H.T., Klitgaard, A.B., Best, M., Thollesson, M., Tendal, O.S., 2013. Taxonomy, biogeography and DNA barcodes of *Geodia* species (Porifera, Demospongiae,

Tetractinellida) in the Atlantic boreo-arctic region. Zool. J. Linn. Soc. 169, 251–311. https://doi.org/10.1111/zoj.12056

Cherkis, N.Z., Steinmetz, S., Schreiber, R., Thiede, J., Theiner, J., 1994. Vesteris Seamount: An enigma in the Greenland Basin. Mar. Geophys. Res. 16, 287–301. https://doi.org/10.1007/BF01224746

Chu, J.W.F., Nephin, J., Georgian, S., Knudby, A., Rooper, C., Gale, K.S.P., 2019. Modelling the environmental niche space and distributions of cold-water corals and sponges in the Canadian northeast Pacific Ocean. Deep. Res. Part I Oceanogr. Res. Pap. 151, 103063. https://doi.org/10.1016/j.dsr.2019.06.009

Clark, M.R., Bernardino, A.F., Roberts, J.M., Narayanaswamy, B.E., Snelgrove, P.V.R., Tuhumwire, J.T., 2021. The Second World Ocean Assessment, in: The Second World Ocean Assessment. United Nations, New York, pp. 439–451.

Clark, M.R., Rowden, A.A., Schlacher, T., Williams, A., Consalvey, M., Stocks, K.I., Rogers, A.D., O'Hara, T.D., White, M., Shank, T.M., Hall-Spencer, J.M., 2010. The Ecology of seamounts: Structure, function, and human impacts. Ann. Rev. Mar. Sci. 2, 253–278. https://doi.org/10.1146/annurev-marine-120308-081109

Clarke, K.R., Gorley, R.N., 2015. Primer v7: User manual v7a.

Clarke, K.R., Warwick, R.M., 2001. Change in marine communities: an approach to statistical analysis and interpretation. 2nd edition. Primer-E, Plymouth. Plymouth, United Kingsom Prim. 172.

Costello, M.J., 2009. Distinguishing marine habitat classification concepts for ecological data management. Mar. Ecol. Prog. Ser. 397, 253–268. https://doi.org/10.3354/meps08317

Costello, M.J., Zhao, Q., Jayathilake, D.R.M., 2020. Defining marine spatial units: Realms, biomes, ecosystems, seascapes, habitats, biotopes, communities and guilds, Encyclopedia of the World's Biomes. Elsevier Inc. https://doi.org/10.1016/B978-0-12-409548-9.12515-1

Davies, A.J., Duineveld, G.C.A., Lavaleye, M.S.S., Bergman, M.J.N., Van Haren, H., 2009. Downwelling and deep-water bottom currents as food supply mechanisms to the cold-water coral *Lophelia pertusa* (Scleractinia) at the Mingulay Reef complex. Limnol. Oceanogr. 54, 620–629. https://doi.org/10.4319/lo.2009.54.2.0620

Davies, C.E., Moss, D., 2004. EUNIS Habitat classification marine habitat types: Revised classification and criteria. Cent. Ecol. Hydrol. 44, 84.

Davies, J.S., Stewart, H.A., Narayanaswamy, B.E., Jacobs, C., Spicer, J., Golding, N., Howell, K.L., 2015. Benthic assemblages of the Anton Dohrn Seamount (NE Atlantic): Defining deep-sea biotopes to support habitat mapping and management efforts with a focus on vulnerable marine ecosystems. PLoS One 10, 1–23. https://doi.org/10.1371/journal.pone.0124815

Davison, J.J., van Haren, H., Hosegood, P., Piechaud, N., Howell, K.L., 2019. The distribution of deep-sea sponge aggregations (Porifera) in relation to oceanographic processes in the Faroe-Shetland Channel. Deep. Res. Part I Oceanogr. Res. Pap. 146, 55–61. https://doi.org/10.1016/j.dsr.2019.03.005

Dunn, D.C., Van Dover, C.L., Etter, R.J., Smith, C.R., Levin, L.A., Morato, T., Colaço, A., Dale, A.C., Gebruk, A. V., Gjerde, K.M., Halpin, P.N., Howell, K.L., Johnson, D., Perez, J.A.A., Ribeiro, M.C., Stuckas, H., Weaver, P., 2018. A strategy for the conservation of biodiversity on mid-ocean ridges from deep-sea mining. Sci. Adv. 4, 1–16. https://doi.org/10.1126/sciadv.aar4313

Durden, J.M., Schoening, T., Althaus, F., Friedman, A., Garcia, R., Glover, A.D., Greinert, J., Jacobsen-Stout, N., Jones, D.O.B., Jordt, A., Kaeli, J.W., Köser, K., Kuhnz, L.A., Lindsay, D., Morris, K.J., Nattkemper, T.W., Osterloff, J., Ruhl, H.A., Singh, H., Tran, M., Bett, B.J., 2016. Perspectives in visual imaging for marine biology and ecology: from acquistion to understanding. Oceanogr. Mar. Biol. An Annu. Rev. 54, 1–72.

Eilertsen, M.H., Georgieva, M.N., Kongsrud, J.A., Linse, K., Wiklund, H., Glover, A.G., Rapp, H.T., 2018. Genetic connectivity from the Arctic to the Antarctic: *Sclerolinum contortum* and *Nicomache lokii* (Annelida) are both widespread in reducing environments. Sci. Rep. 8, 4810 (2018). https://doi.org/10.1038/s41598-018-23076-0

Eilertsen, M.H., Dahlgren, T.G., Rapp, H.T., 2020. A new species of Osedax (Siboglinidae: Annelida) from colonization experiments in the Arctic deep sea. Front. Mar. Sci. 7:443. https://doi.org/10.3389/fmars.2020.00443

EMODnet Bathymetry Consortium (2020). EMODnet Digital Bathymetry (2020). doi:10.12770/bb6a87dd-e579-4036-abe1-e649cea9881a. Available online at: https://www.emodnet-bathymetry.eu/data-products/acknowledgement-in-publications

Environmental Systems Research Institute (ESRI), 2017. ArcGIS Release 10.6. Redlands, CA: ESRI.

EUNIS, 2019. EUNIS marine habitats classification 2019 with crosswalks to Annex I in separate rows. Accessed 16 March 2022. Downloaded from: https://www.eea.europa.eu/data-and-maps/data/eunis-habitat-classification-1/eunis-marine-habitat-classification-review-2019/eunis-marine-habitats-classification-2019.

FAO, 2009. International Guidelines for the Management of deep-sea fisheries in the High Seas. Rome: Food and Agriculture Organization.

Field, J., Clarke, K., Warwick, R., 1982. A practical strategy for analysing multispecies distribution patterns. Mar. Ecol. Prog. Ser. 8, 37–52. https://doi.org/10.3354/meps008037

Goode, S.L., Rowden, A.A., Bowden, D.A., Clark, M.R., 2021. Fine-scale mapping of mega-epibenthic communities and their patch characteristics on two New Zealand seamounts 8, 1–21. https://doi.org/10.3389/fmars.2021.765407

Gotelli, N.J., Colwell, R.K., 2001. Quantifying biodiversity: Procedures and pitfalls in the measurement and comparison of species richness. Ecol. Lett. 4, 379–391. https://doi.org/10.1046/j.1461-0248.2001.00230.x

Hanz, U., Riekenberg, P., de Kluijver, A., van der Meer, M., Middelburg, J.J., de Goeij, J.M., Bart, M.C., Wurz, E., Colaço, A., Duineveld, G.C.A., Reichart, G.-J., Rapp, H.T., Mienis, F., 2022. The important role of sponges in carbon and nitrogen cycling in a deep-sea biological hotspot. Funct. Ecol. 36, 2188–2199. https://doi.org/https://doi.org/10.1111/1365-2435.14117

Hanz, U., Roberts, E.M., Duineveld, G., Davies, A., van Haren, H., Rapp, H.T., Reichart, G.J., Mienis, F., 2021. Long – term observations reveal environmental conditions and food supply mechanisms at an Arctic deep-sea sponge ground. J. Geophys. Res. Ocean. 126, 1–18. https://doi.org/10.1029/2020JC016776

Henrich, R., Hartmann, M., Reitner, J., Schäfer, P., Freiwald, A., Steinmetz, S., Dietrich, P., Thiede, J., 1992. Facies belts and communities of the arctic Vesterisbanken Seamount (Central Greenland Sea). Facies 27, 71–103. https://doi.org/10.1007/BF02536805

Hogg, M.M., Tendal, O.S., Conway, K.W., Pomponi, S.A., Van Soest, R.W.M., Gutt, J., Krautter, M., Roberts, J.M., 2010. Deep-sea sponge grounds Regional Seas, Governance An International Journal Of Policy And Administration.

Hopkins, T.S., 1991. The GIN Sea-A synthesis of its physical oceanography and literature review 1972-1985. Earth Sci. Rev. 30, 175–318. https://doi.org/10.1016/0012-8252(91)90001-V

Horton, T., Marsh, L., Bett, B.J., Gates, A.R., Jones, D.O.B., Benoist, N.M.A., Pfeifer, S., Simon-

963 Lledó, E., Durden, J.M., Vandepitte, L., Appeltans, W., 2021. Recommendations for the
964 standardisation of open taxonomic nomenclature for image-based identifications. Front. Mar.
965 Sci. 8. https://doi.org/10.3389/fmars.2021.620702
966 Howell, K.L., Piechaud, N., Downie, A.L., Kenny, A., 2016. The distribution of deep-sea sponge
967 aggregations in the North Atlantic and implications for their effective spatial management.
968 Deep. Res. Part I Oceanogr. Res. Pap. 115, 203–220.
969 https://doi.org/10.1016/j.dsr.2016.07.005
970 ICES, 2020. ICES/NAFO joint working group on deep-water ecology (WGDEC).
971 https://doi.org/https://doi.org/10.17895/ices.pub.7503
972 Jaeschke, A., Jørgensen, S.L., Bernasconi, S.M., Pedersen, R.B., Thorseth, I.H., Früh-Green, G.L.,
973 2012. Microbial diversity of Loki's Castle black smokers at the Arctic Mid-Ocean Ridge.
974 Geobiology, 10: 548-561. https://doi.org/10.1111/gbi.12009
975 Jeansson, E., Olsen, A., Jutterström, S., 2017. Arctic Intermediate Water in the Nordic Seas, 1991–
976 2009. Deep. Res. Part I Oceanogr. Res. Pap. 128, 82–97.
977 https://doi.org/10.1016/j.dsr.2017.08.013
978 JNCC, 2015. The Marine Habitat Classification for Britain and Ireland Version 15.03. Accessed
979 16 March 2022. Available from: https://mhc.jncc.gov.uk/
980 Klitgaard, A.B., Tendal, O.S., 2004. Distribution and species composition of mass occurrences of
981 large-sized sponges in the northeast Atlantic. Prog. Oceanogr. 61, 57–98.
982 https://doi.org/10.1016/j.pocean.2004.06.002
983 Knudby, A., Kenchington, E., Murillo, F.J., 2013. Modeling the distribution of *Geodia* sponges
984 and sponge grounds in the Northwest Atlantic. PLoS One 8.
985 https://doi.org/10.1371/journal.pone.0082306
986 Kongsrud, J.A., Eilertsen, M.H., Alvestad, T., Kongshavn, K., Rapp, H.T., 2017. New species of
987 Ampharetidae (Annelida: Polychaeta) from the Arctic loki castle vent field. Deep. Res. Part
988 II. 137, 232-245. https://doi.org/10.1016/j.dsr2.2016.08.015
989 Langenkämper, D., Zurowietz, M., Schoening, T., Nattkemper, T.W., 2017. BIIGLE 2.0 -
990 browsing and annotating large marine image collections. Front. Mar. Sci. 4, 1–10.
991 https://doi.org/10.3389/fmars.2017.00083
992 Liu, F., Daewel, U., Samuelsen, A., Brune, S., Hanz, U., Pohlmann, H., Baehr, J., Schrum, C.,
993 2021. Can environmental conditions at North Atlantic deep-Sea habitats be predicted several

994 years ahead? ——Taking sponge habitats as an example. Front. Mar. Sci. 8, 1–22.
995 https://doi.org/10.3389/fmars.2021.703297
996 Maldonado, M., Aquilar, R., Bannister, R.J., Bell, J.J., Conway, K.W., Dayton, P.K., Díaz, C.,
997 Gutt, J., Kelly, M., Kenchington, E.L.R., Leys, S.P., Pomponi, S.A., Rapp, H.T., Rützler, K.,
998 Tendal, O.S., Vacelet, J., Young, C.M., 2016. Sponge grounds as key marine habitats: A
999 synthetic review of types, structure, functional roles, and conservation efforts, Marine Animal
1000 Forests. https://doi.org/10.1007/978-3-319-17001-5
1001 Marine Protection Atlas, Marine Conservation Insitute. Svalbard and Jan Mayen Marine Protected
1002 Areas. Accessed 12 January 2022. Downloaded from: https://mpatlas.org/countries/SJM
1003 Mayer, M., Piepenburg, D., 1996. Epibenthic community patterns on the continental slope off East
1004 Greenland at 75 N. Mar. Ecol. Prog. Ser. 143, 151–164. https://doi.org/10.3354/meps143151
1005 McArthur, M.A., Brooke, B.P., Przeslawski, R., Ryan, D.A., Lucieer, V.L., Nichol, S., McCallum,
1006 A.W., Mellin, C., Cresswell, I.D., Radke, L.C., 2010. On the use of abiotic surrogates to
1007 describe marine benthic biodiversity. Estuar. Coast. Shelf Sci. 88, 21–32.
1008 https://doi.org/10.1016/j.ecss.2010.03.003
1009 Mertz, D.F., Renne, P.R., 1995. Quarternary multi-stage alkaline volcanism at Vesteris Seamount
1010 (Norwegian-Greenland Sea): evidence from laser step heating 40Ar/39Ar experiments. J.
1011 Geodyn. 19, 79–95. https://doi.org/10.1016/0264-3707(94)E0001-B
1012 Meyer, H.K., Roberts, E.M., Mienis, F., Rapp, H.T., 2020. Drivers of megabenthic community
1013 structure in one of the world's deepest silled-fjords, Sognefjord (Western Norway). Front.
1014 Mar. Sci. 7. https://doi.org/10.3389/fmars.2020.00393
1015 Meyer, H.K., Roberts, E.M., Rapp, H.T., Davies, A.J., 2019. Spatial patterns of arctic sponge
1016 ground fauna and demersal fish are detectable in autonomous underwater vehicle (AUV)
1017 imagery. Deep. Res. Part I Oceanogr. Res. Pap. 153, 103137.
1018 https://doi.org/10.1016/j.dsr.2019.103137
1019 Meyer, K.S., Soltwedel, T., Bergmann, M., 2014. High biodiversity on a deep-water reef in the
1020 eastern Fram Strait. PLoS One 9, 1–16. https://doi.org/10.1371/journal.pone.0105424
1021 Miller, K.A., Thompson, K.F., Johnston, P., Santillo, D., 2018. An overview of seabed mining
1022 including the current state of development, environmental impacts, and knowledge gaps.
1023 Front. Mar. Sci. 4. https://doi.org/10.3389/fmars.2017.00418
1024 Morganti, T.M., Slaby, B.M., de Kluijver, A., Busch, K., Hentschel, U., Middelburg, J.J., Grotheer,

H., Mollenhauer, G., Dannheim, J., Tore Rapp, H., Purser, A., Boetius, A., 2022. Giant sponge grounds of Central Arctic seamounts are associated with extinct seep life. Nat. Commun. https://doi.org/10.1038/s41467-022-28129-7

Morrison, K.M., Meyer, H.K., Roberts, E.M., Rapp, H.T., Colaço, A., Pham, C.K., 2020. The first cut is the deepest: Trawl effects on a deep-sea sponge ground are pronounced four years on. Front. Mar. Sci. 7, 1–13. https://doi.org/10.3389/fmars.2020.605281

Murillo, F.J., Kenchington, E., Tompkins, G., Beazley, L., Baker, E., Knudby, A., Walkusz, W., 2018. Sponge assemblages and predicted archetypes in the eastern Canadian Arctic, Marine Ecology Progress Series.

Nilsson-Cantell C-A. 1978. Cirripedia Thoracica and Acrothoracica. Oslo: Universitetsforlaget; p. 133.

Oljedirektoratet, 2021. Åpningsprosess for undersøkelse og utvinning av havbunnsmineraler på norsk kontinentalsokkel Forslag til program for konsekvensutredning etter havbunnsmineralloven. (In Norwegian).

Olsen, B. R., Økland, I. E., Thorseth, I. H., Pedersen, R. B., and Rapp, H. T., 2016. Environmental challenges related to offshore mining and gas hydrate extraction. Norway: Norwegian Environment Agency.

Ooms, J., 2021. magick: Advanced Graphics and Image-Processing in R. R package version 2.6.0. https://CRAN.R-project.org/package=magick.

Parry, M.. E.V.E. V, Howell, K.L., Narayanaswamy, B.E., Bett, B.J., Jones, D.O.B., Hughes, D.J., Piechaud, N., Nickell, T.D., Ellwood, H., Askew, N., Jenkins, C., Manca, E., Jones, B., Hughes, D.J., Piechaud, N., Nickell, T.D., Ellwood, H., Askew, N., Jenkins, C., Manca, E., 2015. A deep-sea section for the marine habitat classification of Britain and Ireland v15.03. Peterborough.

Pedersen, R.B., Bjerkgård, T., 2016. Sea-floor massive sulphides in Arctic Waters, in: Mineral Resources In The Arctic 1. pp. 209–216.

Pedersen, R.B., Olsen, B.R., Barreyre, T., Bjerga, A., Denny, A., Heggernes Eilertsen, M., Fer, I., Haflidason, H., Hestetun, J.T., Jørgensen, S., Steen, I.H., Stubseid, H., Tandberg, A.H.S., Thorseth, I.H., 2021. Fagutredning mineralressurse i Norskehavet landskapstrekk, naturtyper og benthiske økosystemer. Bergen. (In Norwegian).

Pedersen, R.B., Rapp, H.T., Thorseth, I.H., Lilley, M.D., Barriga, F.J.A.S., Baumberger, T.,

Flesland, K., Fonseca, R., Früh-Green, G.L., Jorgensen, S.L., 2010a. Discovery of a black smoker vent field and vent fauna at the Arctic Mid-Ocean Ridge. Nat. Commun. 1. https://doi.org/10.1038/ncomms1124

Pedersen, R.B., Thorseth, I.H., Nygård, T.E., Lilley, M.D., Kelley, D.S., 2010b. Hydrothermal activity at the Arctic Mid-Ocean Ridges, in: Rona, P.A., Devey, C.W., Dyment, J., Murton, B.J. (Eds.), Diversity of Hydrothermal Systems on Slow Spreading Ocean Ridges. pp. 67–89. https://doi.org/10.1029/2008GM000783

Perez, J.A.A., Kitazato, H., Sumida, P.Y.G., Sant'Ana, R., Mastella, A.M., 2018. Benthopelagic megafauna assemblages of the Rio Grande Rise (SW Atlantic). Deep. Res. Part I Oceanogr. Res. Pap. 134, 1–11. https://doi.org/10.1016/j.dsr.2018.03.001

Piepenburg, D., 2005. Recent research on Arctic benthos: Common notions need to be revised. Polar Biol. 28, 733–755. https://doi.org/10.1007/s00300-005-0013-5

Piepenburg, D., Schmid, M.K., 1996. Distribution, abundance, biomass, and mineralization potential of the epibenthic megafauna of the Northeast Greenland shelf. Mar. Biol. 125, 321–332. https://doi.org/10.1007/BF00346313

Ramirez-Llodra, E., Hilario, A., Paulsen, E., Costa, C.V., Bakken, T., Johnsen, G., Rapp, H.T., 2020. Benthic communities on the Mohn's Treasure Mound: Implications for management of seabed mining in the Arctic Mid-Ocean Ridge. Front. Mar. Sci. 7, 1–12. https://doi.org/10.3389/fmars.2020.00490

Ramiro-Sánchez, B., González-Irusta, J.M., Henry, L.-A., Cleland, J., Yeo, I., Xavier, J.R., Carreiro-Silva, M., Sampaio, Í., Spearman, J., Victorero, L., Messing, C.G., Kazanidis, G., Roberts, J.M., Murton, B., 2019. Characterization and mapping of a deep-sea sponge ground on the Tropic Seamount (Northeast Tropical Atlantic): Implications for spatial management in the High Seas. Front. Mar. Sci. 6. https://doi.org/10.3389/fmars.2019.00278

Ramos, M., Bertocci, I., Tempera, F., Calado, G.G., Albuquerque, M.M., Duarte, P., 2016. Patterns in megabenthic assemblages on a seamount summit (Ormonde Peak, Gorringe Bank, Northeast Atlantic). Mar. Ecol. 37, 1057–1072. https://doi.org/10.1111/maec.12353

Rice, A.L., Thurston, M.H., New, A.L., 1990. Dense aggregations of a hexactinellid sponge, *Pheronema carpenteri*, in the Porcupine Seabight (northeast Atlantic Ocean), and possible causes. Prog. Oceanogr. 24, 179–196.

Riisgård, H.U., 2015. Filter-feeding Mechanisms in Crustaceans. Nat. Hist. Crustac. Vol. 2 -

Lifestyles Feed. Biol. 418–463.

Roberts, E.M., Bowers, D.G., Meyer, H.K., Samuelsen, A., Rapp, H.T., Cárdenas, P., 2021. Water masses constrain the distribution of deep-sea sponges in the North Atlantic Ocean and Nordic Seas. Mar. Ecol. Prog. Ser. 659, 75–96. https://doi.org/10.3354/meps13570

Roberts, E.M., Mienis, F., Rapp, H.T., Hanz, U., Meyer, H.K., Davies, A.J., 2018. Oceanographic setting and short-timescale environmental variability at an Arctic seamount sponge ground. Deep. Res. Part I Oceanogr. Res. Pap. 138, 98–113. https://doi.org/10.1016/j.dsr.2018.06.007

Rogacheva, A. V., Mironov, A.N., Minin, K. V., Gebruk, A. V., 2013. Morphological evidence of depth-related speciation in deep-sea Arctic echinoderms. Invertebr. Zool. 10, 143–166. https://doi.org/10.15298/invertzool.10.1.07

Rogers, A.D., 2018. The Biology of Seamounts: 25 Years on, 1st ed, Advances in Marine Biology. Elsevier Ltd. https://doi.org/10.1016/bs.amb.2018.06.001

Rogers, A.D., Baco, A., Griffiths, H., Hart, T., Hall-Spencer, J., 2007. Corals on seamounts, in: Pitcher, T.J., Morato, T., Hart, P.J.B., Clark, M.R., Haggan, N., Santos, R.S. (Eds.), Seamounts: Ecology, Fisheries & Conservation. Blackwell Publishing, Oxford, pp. 1–527. https://doi.org/10.1002/9780470691953

Ross, R.E., Howell, K.L., 2013. Use of predictive habitat modelling to assess the distribution and extent of the current protection of "listed" deep-sea habitats. Divers. Distrib. 19, 433–445. https://doi.org/10.1111/ddi.12010

Samadi, S., Bottan, L., Macpherson, E., De Forges, B.R., Boisselier, M.C., 2006. Seamount endemism questioned by the geographic distribution and population genetic structure of marine invertebrates. Mar. Biol. 149, 1463–1475. https://doi.org/10.1007/s00227-006-0306-4

Samadi, S., Schlacher, T.A., de Forges, B.R., 2007. Seamount benthos, in: Pitcher, T.J., Morato, T., Hart, P.J.B., Clark, M.R., Haggan, N., Santos, R.S. (Eds.), Seamounts: Ecology, Fisheries and Conservation. Blackwell Publishing, Oxford, pp. 119–140.

Sánchez, F., Serrano, A., Ballesteros, M.G., 2009. Photogrammetric quantitative study of habitat and benthic communities of deep Cantabrian Sea hard grounds. Cont. Shelf Res. 29, 1174–1188. https://doi.org/10.1016/j.csr.2009.01.004

Sánchez, F., Serrano, A., Parra, S., Ballesteros, M., Cartes, J.E., 2008. Habitat characteristics as determinant of the structure and spatial distribution of epibenthic and demersal communities

of Le Danois Bank (Cantabrian Sea, N. Spain). J. Mar. Syst. 72, 64–86. https://doi.org/10.1016/j.jmarsys.2007.04.008

Schander, C., Rapp, H.T., Kongsrud, J.A., Bakken, T., Berge, J., Cochrane, S., Oug, E., Byrkjedal, I., Todt, C., Cedhagen, T., Fosshagen, A., Gebruk, A., Larsen, K., Levin, L., Obst, M., Pleijel, F., Stöhr, S., Warén, A., Mikkelsen, N.T., Hadler-Jacobsen, S., Keuning, R., Petersen, K.H., Thorseth, I.H., Pedersen, R.B., 2010. The fauna of hydrothermal vents on the Mohn Ridge (North Atlantic). Mar. Biol. Res. 6:2, 155-171. https://doi.org/10.1080/17451000903147450

Schoening, T., Bergmann, M., Ontrup, J., Taylor, J., Dannheim, J., Gutt, J., Purser, A., Nattkemper, T.W., 2012. Semi-automated image analysis for the assessment of megafaunal densities at the Artic deep-sea observatory HAUSGARTEN. PLoS One 7, 1–14. https://doi.org/10.1371/journal.pone.0038179

Sswat, M., Gulliksen, B., Menn, I., Sweetman, A.K., Piepenburg, D., 2015. Distribution and composition of the epibenthic megafauna north of Svalbard (Arctic). Polar Biol. 38, 861–877. https://doi.org/10.1007/s00300-015-1645-8

Steen, I.H., Dahle, H., Stokke, R., Roalkvam, I., Daae, F.L., Rapp, H.T., Pedersen, R.B., Thorseth, I.H., 2016. Novel barite chimneys at the Loki's Castle Vent Field shed light on key factors shaping microbial communities and functions in hydrothermal systems. Front. Microbiol. 6, 1–13. https://doi.org/10.3389/fmicb.2015.01510

Unger Moreno, K.A., Thal, J., Bach, W., Beier, C., Haase, K.M., 2021. Volcanic structures and magmatic evolution of the Vesteris Seamount, Greenland Basin. Front. Earth Sci. 9, 1–14. https://doi.org/10.3389/feart.2021.711910

Vad, J., Barnhill, K.A., Kazanidis, G., Roberts, J.M., 2021. Human impacts on deep-sea sponge grounds: Applying environmental omics to monitoring, 1st ed, Advances in Marine Biology. Elsevier Ltd. https://doi.org/10.1016/bs.amb.2021.08.004

Victorero, L., Robert, K., Robinson, L.F., Taylor, M.L., Huvenne, V.A.I., 2018. Species replacement dominates megabenthos beta diversity in a remote seamount setting. Sci. Rep. 8, 1–11. https://doi.org/10.1038/s41598-018-22296-8

Washburn, T.W., Turner, P.J., Durden, J.M., Jones, D.O.B., Weaver, P., Van Dover, C.L., 2019. Ecological risk assessment for deep-sea mining. Ocean Coast. Manag. 176, 24–39. https://doi.org/10.1016/j.ocecoaman.2019.04.014

Watling, L., Auster, P.J., 2021. Vulnerable marine ecosystems, communities, and indicator

species: Confusing concepts for conservation of seamounts. Front. Mar. Sci. 8, 1–7. https://doi.org/10.3389/fmars.2021.622586

Wentworth, C.K., 1922. A scale of grade and class terms for clastic sediments. J. Geol. 30, 377–392. https://doi.org/10.1086/622910

Wurz, E., Beazley, L., MacDonald, B., Kenchington, E., Rapp, H.T., Osinga, R., 2021. The hexactinellid deep-water sponge *Vazella pourtalesii* (Schmidt, 1870) (Rossellidae) copes with temporarily elevated concentrations of suspended natural sediment. Front. Mar. Sci. 8, 1–15. https://doi.org/10.3389/fmars.2021.611539

Yesson, C., Clark, M.R., Taylor, M.L., Rogers, A.D., 2011. The global distribution of seamounts based on 30 arc seconds bathymetry data. Deep. Res. Part I Oceanogr. Res. Pap. 58, 442–453. https://doi.org/10.1016/j.dsr.2011.02.004

Highlights - Beyond the tip of the seamount: Distinct megabenthic communities found beyond the charismatic summit sponge ground on an arctic seamount (Schulz Bank, Arctic Mid-Ocean Ridge) (H.K. Meyer, A.J. Davies, E.M. Roberts, J.R. Xavier, P.A. Ribeiro, H. Glenner, S.-R. Birkely, and H.T. Rapp)

- Distinct biotopes were described and classified on an arctic seamount
- Vulnerable Marine Ecosystem indicator species were found in all biotopes
- Summit of the seamount covered by diverse arctic sponge ground
- Dense sponge aggregations dominated the lower bedrock walls
- Stalked crinoid fields and ophiuroid beds characterised soft bottom regions

Declaration of interests

☒ The authors declare that they have no known competing financial interests or personal relationships that could have appeared to influence the work reported in this paper.

☐ The authors declare the following financial interests/personal relationships which may be considered as potential competing interests: